

PARAMETRIC STUDY OF EROSION WEAR OF SOLID – LIQUID MIXTURE

*A Thesis Report Submitted
in partial fulfillment of the requirements for
the award of degree of*

**MASTER OF ENGINEERING
IN
PRODUCTION AND INDUSTRIAL ENGINEERING**

Submitted by

**Dalbir Singh Dhindsa
Roll No.: 800982003**

Under the Guidance of

**Dr. S.K. Mohapatra
Sr. Professor MED & Dean Academic Affair
Thapar University, Patiala**



**DEPARTMENT OF MECHANICAL ENGINEERING
THAPAR UNIVERSITY
PATIALA-147004, INDIA.**

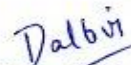
June 2011

DECLARATION

I hereby certify that the work which is being presented in the report entitled, "PARAMETRIC STUDY OF EROSION WEAR OF SOLID – LIQUID MIXTURE", in partial fulfillment of the requirements for the award of degree of Master of Engineering in Mechanical Engineering with specialization in **PRODUCTION AND INDUSTRIAL ENGINEERING** submitted in **Mechanical Engineering Department** of Thapar University, Patiala, is an authentic record of my own work carried out under the supervision of **Dr. S.K. Mohapatra** and refers other researcher's works which are duly listed in the reference section.

The matter presented in this thesis has not been submitted for the award of any other degree of this or any other university.


Date: 15.7.2011


(Dalbir Singh Dhindsa)


Place: Patiala


This is to certify that the above statement made by the candidate is correct and true to the best of my knowledge.

Supervisor:


Dr. S.K. Mohapatra
Dean of Academic Affairs
Thapar University, Patiala

Counter signed by


Dr. Ajay Batish
Professor & head
Mechanical Engineering Department
Thapar University, Patiala


Dr. S.K. Mohapatra
Dean of Academic Affairs
Thapar University, Patiala

ACKNOWLEDGEMENTS

Words are often less to reveal one's deep regards. With an understanding that work like this can never be the outcome of a single person, I take this opportunity to express my profound sense of gratitude and respect to all those who helped me through the duration of this work.

This work would not have been possible without the encouragement and able guidance of supervisor Dr. S.K. Mohapatra. Their enthusiasm and optimism made this experience both rewarding and enjoyable. Most of the novel ideas and solutions in this work are the result of our numerous stimulating discussions. Their feedback and editorial comments were also invaluable for the writing of this thesis. I am grateful to Dr. Ajay Batish, Head of Department of Mechanical Engineering Department for providing me the facilities in the Department for the completion of my work.

I take pride of myself being son of ideal parents for their everlasting desire, sacrifice, affectionate blessings, and help, without which it would not have been possible for me to complete my studies.

I would like to thank Mr. Satish Kumar, Assistant Professor, MED for their novel ideas and solutions in completion of this thesis work.

I am also very grateful to my all friends (Randeep Singh & Mani kanwar Singh Sarao) for accompanying me during the most outstanding year of my life and standing by me in every situation.

I would like to thank to all the faculty members and employees of Mechanical Engineering Department, Thapar University, Patiala for their everlasting support.

Last but not least, I would like to thank God for all good deeds.

Dalbir
(Dalbir Singh Dhindsa)

ABSTRACT

Over the last few decades there has been a phenomenal growth in the demand of raw materials. This rise in demand has led to drastic changes in the existing techniques of mining, food processing, power generation and other sectors where transportation of suspended solids play a major role. Due to this change, there has been an increase in requirements in slurry transportation.

Slurry is a mixture of solids and liquids. The most commonly used liquid is water. Material loss due to erosion wear is a serious problem associated with flow of solid-liquid mixtures. Slurry erosion limits the useful life of equipment and there efficiency. Erosion is therefore a critical parameter for design, selection and operation of the hydraulic transportation system. Engineering interest is to estimate the service life of equipment / components subjected to slurry erosion and to investigate the possibilities of enhancement of their life. As per the application different materials are used.

The present work to study of erosion wear of solid liquid mixture for its different applications. Depending upon applications different materials are selected which are used in pipes, pumps and turbine blades. The materials selected are mild steel, grey cast iron 13Cr4Ni steel and 16Cr5Ni steel. The jet type erosion tester is used to study the erosion wear by bottom ash water solid liquid mixture. The bottom ash required for testing purpose was collected from Guru Govind Singh thermal power plant, Ropar, Punjab. Maximum particle size of solids is 2000μ . The effect of impact angle and effect of flow rate of slurry is evaluated.

CONTENTS

Chapter	Item Description	Page No.
	Contents	i-ii
	List of figures	iii-iv
	List of tables	v
	Abbreviations	vi
1	Introduction	1
1.1	Slurry	1
1.2	1.2.1 Homogeneous flows or Non-Settling slurries	1
	1.2.2 Heterogeneous flows or settling slurries	
1.3	Operating Parameters of Slurry	2
1.4	Transportation of Slurry	3
	1.4.1 Pumps used for transportation of slurries	4
1.5	Wear	5
	1.5.1 Erosive Wear	5
	1.5.2 Mechanism of Erosion Wear	5
	1.5.3 Types of Erosion wear	9
	1.5.4 Parameters affecting on erosion wear	10
1.6	Types of Test Rig	12
1.7	Motivation for Thesis Work	18
2	Literature Review	19
3	Experimental Setup	28
3.1	Description of Jet Erosion Tester	28
3.2	Working of Jet Erosion Tester	30
3.3	Procedure of Evolution of Different Materials	30
3.4	Materials Used	31
4	Properties of Bottom Ash	34
4.1	Bench Scale Test	34
	4.1.1 Particle Size Distribution	34
	4.1.2 Specific gravity	34
	4.1.3 Static Settled Concentration	35
	4.1.4 pH value	35
	4.1.5 Rheological Behavior of Solid-Liquid Mixture	36
4.2	Physical properties of Bottom Ash	37
4.3	SEM Analysis	43

5	Results and Discussion	44
5.1	Erosion of Mild Steel	44
	5.1.1 Weight Loss with respect to Time	44
	5.1.2 Effect of Velocity	46
	5.1.3 Effect of Angle.	46
	5.1.4 SEM analysis of Mild Steel	47
5.2	Erosion of Grey Cast Iron	49
	5.2.1 Weight Loss with respect to Time	49
	5.2.2 Effect of Velocity	51
	5.2.3 Effect of angle.	52
	5.2.4 SEM analysis of Grey Cast Iron	52
5.3	Erosion of 13Cr-4Ni Stainless Steel	54
	5.3.1 Weight Loss with respect to Time	54
	5.3.2 Effect of velocity	56
	5.3.3 Effect of impact angle	57
	5.3.4 SEM analysis of 13Cr- 4Ni Stainless Steel	57
5.4	Erosion of 16Cr-5Ni Stainless Steel	59
	5.4.1 Weight Loss with respect to Time	59
	5.4.2 Effect of velocity	61
	5.4.3 Effect of Impact Angle	62
	5.4.4 SEM analysis of 16Cr-5Ni Stainless Steel	62
5.5	Comparison of the Mild Steel, Grey Cast Iron, 13Cr-4Ni Stainless Steel & 16Cr-5Ni Stainless Steel	64
	5.5.1 Erosion with respect to Time	64
	5.5.2 Erosion with respect to Mass Flow Rate	65
	5.5.3 Erosion with respect to varying Impact Angle	66
6	Conclusions and Future Scope	67

LIST OF FIGURES

Figure No.	Item Description	Page No.
1.1	Homogeneous slurry flow	1
1.2	Heterogeneous slurry flow	2
1.3	Transportation of slurry	3
1.4	Pumps used for transportation of slurry	4
1.5	Cutting Erosion	6
1.6	Ploughing Erosion	6
1.7	Extrusion and Forging Mechanism	7
1.8	Subsurface deformation and Cracking	8
1.9	Miller Test Apparatus	12
1.10	Slurry Pot Tester	13
1.11	Jet Impingement Tester	14
1.12	Falling Jet Test Apparatus	15
1.13	Jet-in-Silt Apparatus	16
1.14	Centrifugal Erosion Tester	17
1.15	Coriolis Erosion Tester	17
3.1	Jet Erosion Tester	29
3.2	Spectrometer	31
3.3	Composition of mild steel by spectrometer	32
3.4	Composition of grey cast iron by spectrometer	32
3.5	Chemical composition of 13/4 steel by spectrometer	33
3.6	Composition of 16/5 steel by spectrometer	33
4.1	Rheometer (Anton Paar, Germany)	36
4.2	Particle size distribution curve of bottom ash sample	40
4.3	Settled concentration curve of bottom ash sample	40
4.4 (a)	Rheology of bottom ash slurry sample with variation of concentration such as 10% bottom ash	41
4.4 (b)	Rheology of bottom ash slurry sample with variation of concentration such as 20% bottom ash	41
4.4 (c)	Rheology of bottom ash slurry sample with variation of concentration such as 30% bottom ash	41
4.4 (d)	Rheology of bottom ash slurry sample with variation of concentration such as 40% bottom ash	42
4.4 (e)	Rheology of bottom ash slurry sample with variation of concentration such as 50% bottom ash	42
4.5	SEM analysis of bottom ash	43

5.1	Weight Loss w.r.t Time	44
5.2	Weight Loss w.r.t Time	45
5.3	Weight Loss w.r.t Time	45
5.4	Effect of velocity on mild steel	46
5.5	Effect of Angle on Mild Steel	47
5.6	SEM of mild steel before wear	48
5.7	SEM of mild steel after wear	48
5.8	Weight Loss w.r.t Time	49
5.9	Weight Loss w.r.t Time	50
5.10	Weight Loss w.r.t Time	50
5.11	Effect of velocity	51
5.12	Effect of Impact Angle	52
5.13	SEM of grey cast iron before wear	53
5.14	SEM of grey cast iron after wear	53
5.15	Weight Loss w.r.t Time	54
5.16	Weight Loss w.r.t Time	55
5.17	Weight Loss w.r.t Time	55
5.18	Effect of velocity	56
5.19	Effect of Impact Angle	57
5.20	SEM of 13 Cr-4Ni Stainless Steel before wear	58
5.21	SEM of 13 Cr-4Ni Stainless Steel after wear	58
5.22	Weight Loss w.r.t Time	59
5.23	Weight Loss w.r.t Time	60
5.24	Weight Loss w.r.t Time	60
5.25	Weight loss w.r.t Velocity	61
5.26	Effect of Impact Angle	62
5.27	SEM of 16Cr-5Ni Stainless Steel before wear	63
5.28	SEM of 16Cr-5Ni Stainless Steel after wear	63
5.29	Erosion with respect to Time	64
5.30	Erosion with respect to Mass Flow Rate	65
5.31	Erosion with respect to varying Impact Angle	66

LIST OF TABLES

Table No.	Item Description	Page No.
4.1	Rheological Properties of bottom ash at temperature	37
4.2	pH value of slurry	38
4.3	Settled concentration of bottom ash sample	38
4.4	Particle size distribution	39

ABBREVIATIONS

PSD	Particle size distribution
16Cr-5Ni	16 Chromium – 5 Nickel Stainless Steel
13Cr-4Ni	13 Chromium – 4 Nickel Stainless Steel
rpm	Revolutions Per Minute

NOMENCLATURE AND SYMBOLS

Symbol	Description
t	Time, seconds
T	Temperature, °C
%	Percentage
°C	Degree Celsius
mm	Millimeter
µm	Micro meter
W_b	Weight of beaker
W_{bs}	Weight of beaker and solid
W_{bw}	Weight of beaker and water
W_{bsw}	Weight of beaker, solid and water

CHAPTER-1

INTRODUCTION

1.1 SLURRY

Slurry is a mixture of solids and liquids. The most commonly used liquid is water. The physical characteristics of the slurry are dependent on many factors such as size and distribution of solid particles, level of turbulence, temperature, and absolute (or dynamic) viscosity of the carrier fluid. Single-phase liquids are allowed to flow at slow speeds from a laminar flow to a turbulent flow but in slurry flows, the flow must overcome a deposition critical velocity or a viscous transition critical velocity. If the speed of flow is not sufficiently high, the particles will not be maintained in suspension.

1.2 TYPESS OF SLURRY FLOWS

Based on the solid fluid interaction slurry flows are divided into two different types:

1.2.1 Homogeneous flows or Non-Settling slurries

In homogeneous flows solids are uniformly distributed throughout the liquid carrier. For example, copper concentrate slurry after undergoing a process of grinding and thickening, drilling mud, sewage sludge, and fine limestone behave as homogeneous flows. Figure 1.1 shows the distribution of solid particles in homogeneous flows.

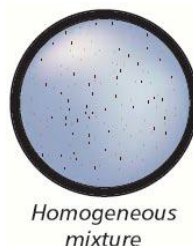


Figure 1.1: Homogeneous slurry flow

1.2.2 Heterogeneous flows or settling slurries

In heterogeneous flows, solids are not uniformly mixed in the horizontal plane. Heavier particles tend to settle down and lighter particles tend to float. Sliding bed may form in the pipe, with the heavier particles at the bottom and the lighter ones in suspension. Heterogeneous slurries are encountered in many places mining, phosphate rock mining, and dredging applications. Heterogeneous flows require a minimum carrier velocity. Figure 1.2 shows the distribution of solid particles in heterogeneous flows.



*Heterogeneous
mixture, partly
stratified*

Figure 1.2: Heterogeneous slurry flow

1.3 OPERATING PARAMETERS OF SLURRY

- **Apparent viscosity:** It is defined as the property of the fluid resistance offered to the flow.
- **Critical carrying velocity:** It is defined as the mean velocity of the specific slurry in a particular conduit, above which the solids phase remains in suspension, and below which solid-liquid Separation occurs.
- **Effective particle diameter:** Effective particle diameter is the single or average particle size used to represent the behavior of a mixture of various sizes of particles in slurry. This designation is used to calculate system requirements and pump performance.
- **Concentration of solids by volume:** The actual volume of the solid material in a given volume of slurry, divided by the given volume of slurry, multiplied by 100.
- **Concentration of solids by weight:** The weight of dry solids in a given volume of slurry, divided by the total weight of the slurry, multiplied by 100.
- **Settling slurry:** Slurry in which the solids will move to the bottom of the containing vessel or conduit at a discernible rate, but which will remain in suspension if the slurry is agitated constantly.

- **Settling velocity:** It is the rate at which the solids in slurry will move to the bottom of stationary container.
- **Yield value (Stress):** It is the value of stress at which slurries will start to deform and under this value there will be no relative motion between adjacent particles in the slurry.

1.4 TRANSPORTATION OF SLURRY

Over the last few decades there has been a phenomenal growth in the demand of raw materials. This rise in demand has led to drastic changes in the existing techniques of mining, food processing, power generation and other sectors where transportation of suspended solids play a major role. Due to this change, there has been an increase in requirements in slurry transportation. A typical slurry transport system is shown in the Figure 1.3. Pump plays a vital role in transportation of slurry; different types of pumps are available for slurry transportation, but centrifugal pumps are most widely used in slurry transportation applications due to the following reasons :-

- Higher flow rates can be obtained.
- Pulse free flow can be obtained.
- Lower initial and maintenance cost of positive displacement pumps.
- Solid particle of any size can be transported.

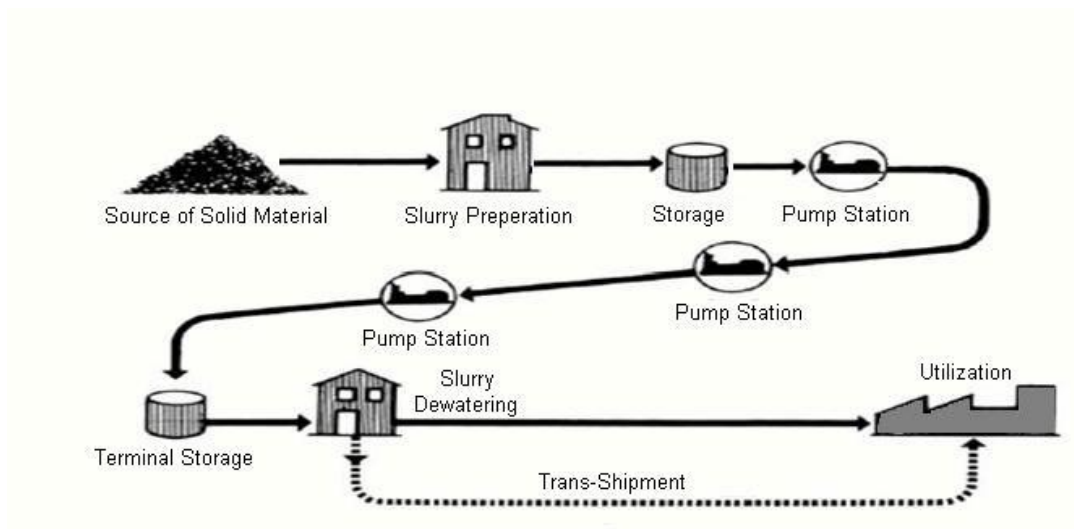


Figure 1.3: Transportation of slurry

1.4.1 Pumps used for transportation of slurries

The choice of pumps or pumping systems for slurry transport will depend not only on the flow, head required, suction conditions, type of installation and location, as for any other pump application, but also on the slurry flow regime and properties. Roto-Dynamic pumps, of which the centrifugal or radial-flow type is the most common in slurry service, are usually considered for the higher flow and lower head duties. However, positive-displacement and reciprocating types are tend to be used for the lower flow and high pressure applications, e.g. long-distance pipelines. However, relatively high pressures may also be achieved with centrifugal pumps, depending on casing pressure limitations, by arranging them in series. For a given duty, centrifugal pumps are usually cheaper, occupy less space and have lower maintenance costs than positive displacement types, and can handle much larger solids. Figure 1.4 gives us a pictorial idea of pump application depending upon discharge and particle size required.

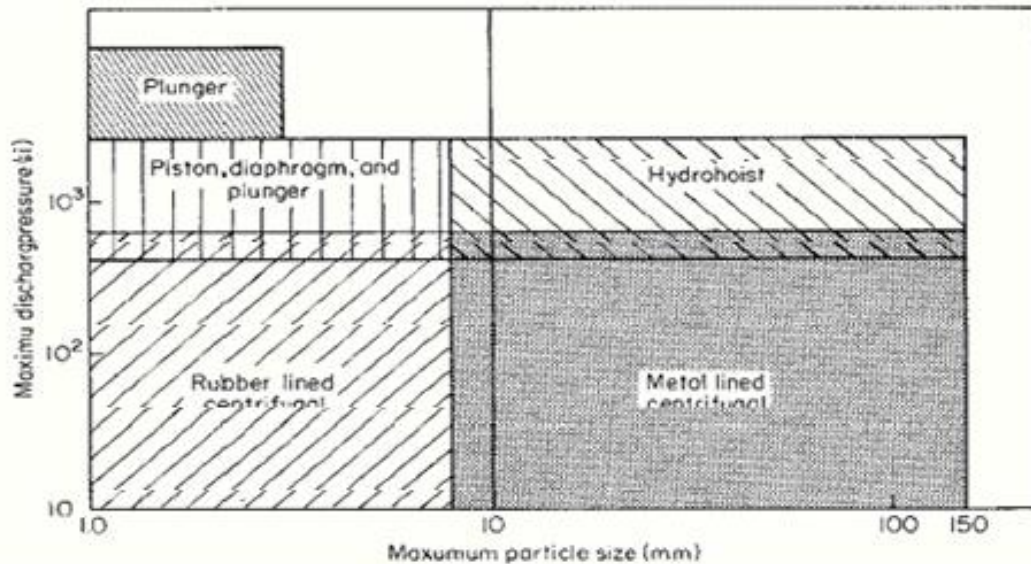


Figure 1.4: Pumps used for transportation of slurries

1.5 WEAR

Wear is defined as the progressive volume loss of material from a target surface. It may occur due to corrosion, abrasion or erosion. The wear due to corrosion is caused by chemical reactions, which can be prevented by adopting suitable measures, whereas the wear due to abrasion and/or erosion can only be minimized by controlling the affecting parameters.

1.5.1 Erosive Wear

Erosive wear is the dominant process which can be defined as the removal of material from a solid surface. It is due to mechanical interaction between the surface and the impinging particles in a liquid stream. In Erosion process there is a transfer of kinetic energy to the surface. With the increase in kinetic energy of the particles impacting at the target surface, it leads to increase in the material loss due to erosion. It depends on the predominant impact angle of particle impingement with the material surface and it will vary from 0 to 90 degrees. Impact angle depend on both fluid particle and particle - particle interaction. This type of wear can be practically found in slurry pumps, angled pipe bends, turbines, pipes and pipe fitting, nozzles, burners etc. The material loss due to erosion increases with the increase in kinetic energy of the particles impacting at the target surface. The volume loss due to erosion is a troublesome problem for slurry transportation systems e.g. mineral transport systems, ash disposal systems. The erosion wear due to the air borne particles in some devices such as jet planes and turbines is also significant due to very high impact velocity.

1.5.2 Mechanism of Erosion Wear

The commonly accepted erosion mechanisms are classified as:

1. Cutting
2. Ploughing
3. Extrusion and forging
4. Subsurface deformation and cracking

1. Cutting Erosion

If the particles are very sharp it causes cutting erosion and a micromachining action occurs when particles interact with the material surface. Minimal plastic deformation of the surface region occurs in slurry pipeline because of two mechanisms namely, corrosion and erosion. These mechanisms are quite different in various manners

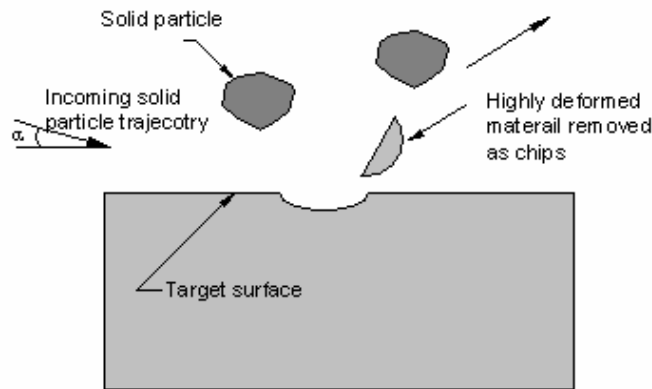


Figure 1.5: Cutting Erosion

2. Ploughing Erosion

Ploughing erosion is a two stage process involving localized plastic deformation of the surface from rounded particle impacts. In first stage process, particle impacts form surface craters with plastic flow of the surface occurring around the particle edges during impact. As a result of the particle collision, an extruded shear lip is formed. The second stage process involves repeated particle impacts causing fatigue of the extruded shear lip regions. The shear lips fail and are broken off.

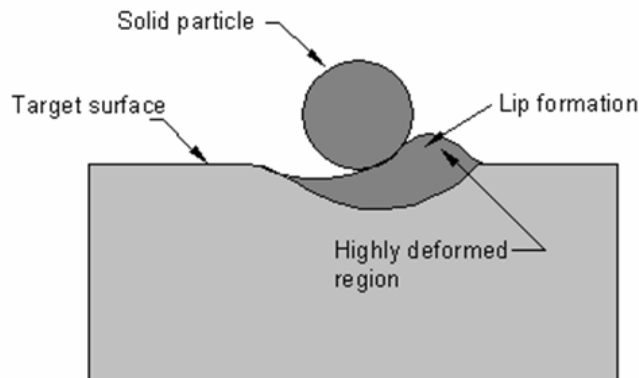


Figure 1.6: Ploughing Erosion

3. Extrusion and Forging Mechanism

This mechanism is also known as platelet mechanism. The impact of a solid particle spreads the target material over the adjacent crater in the direction of impact. This spread material get further flattened and extended to develop a platelet. A proposed sequence of particle impacts that could cause the material removal due to platelet mechanism is shown.

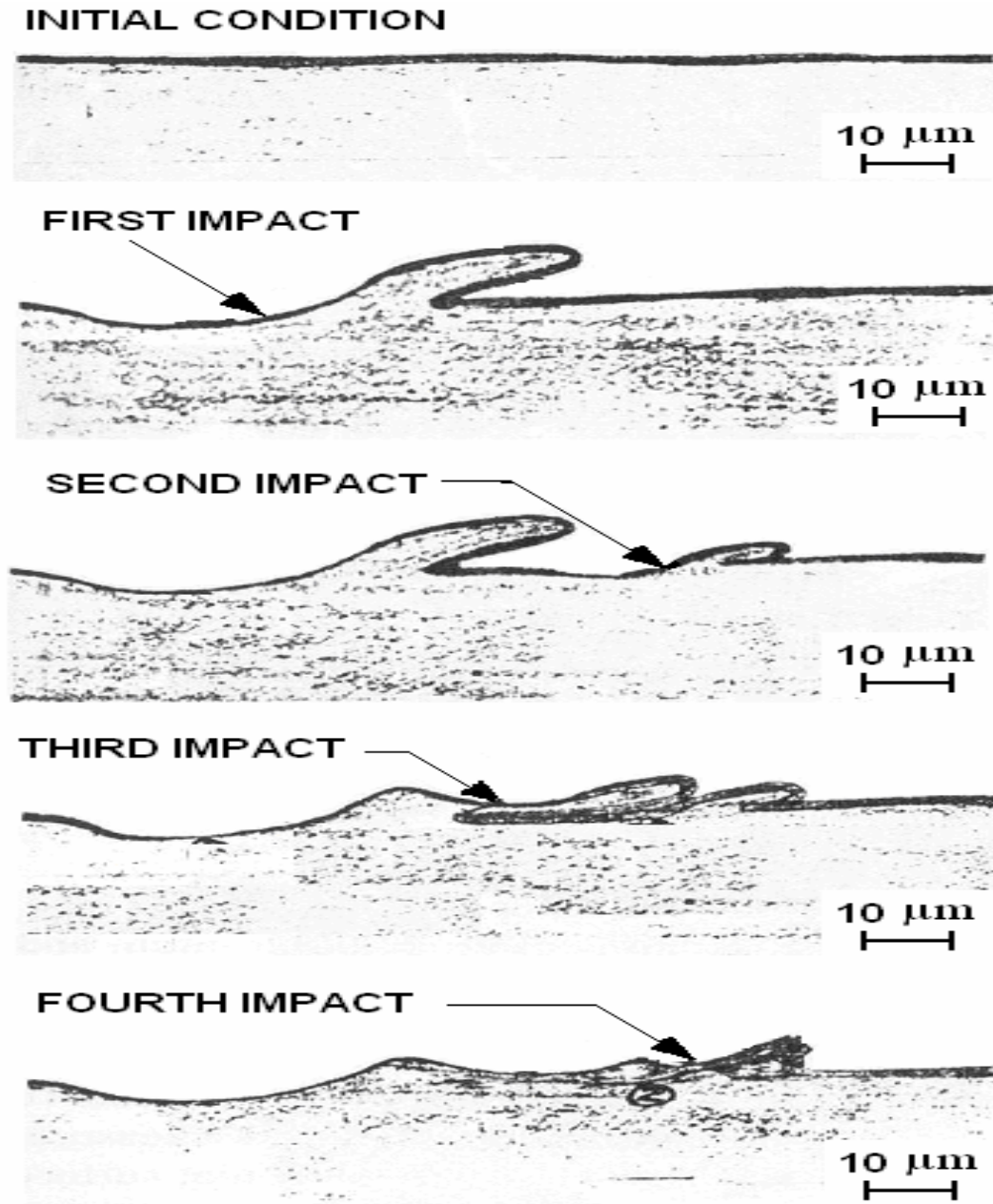


Figure 1.7: Extrusion and Forging Mechanism

4. Subsurface deformation and Cracking

A blunt particle striking the target surface at high velocity causes localized plastic deformation at the point of contact, which develops cracks leading to wear by brittle fracture. This type of wear mechanism is known as subsurface deformation or cracking. As the particle moves over the surface, small increment in the plastic strain takes place and the residual stresses develop in the deformed layer. Since the ratio of particle size to contact asperity size is 100:1, the material experiences cyclic loading and unloading as it moves over the surface. This leads to the anisotropy in the surface layer and subsequent crack generation. When cracks generated from various parts of the solid link together through crack propagation, loose eroded material is formed. The ploughing process also causes subsurface plastic deformation and may also contribute to the generation and propagation of subsurface cracks. When subsurface cracks propagate, the target material loses out as small wear particles causing loss of material from the surface. Thus the solid particle striking at large impact angles causes brittle fracture and the material is removed from the surface by the formation and intersection of cracks as shown in Figure 1.8. The fracture generates the new surface in following two steps:

- i. Cracks and voids can be nucleated at or below the surface
- ii. Cracks will propagate from these nucleated or pre-existing flaws to develop long cracks.

Thus the subsurface damage processes have dominant effect on erosion behavior of materials particularly brittle type.

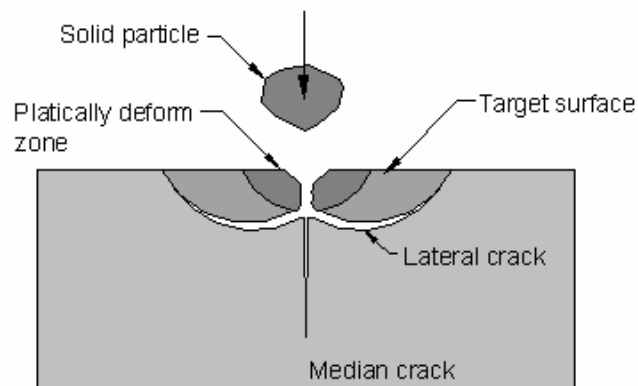
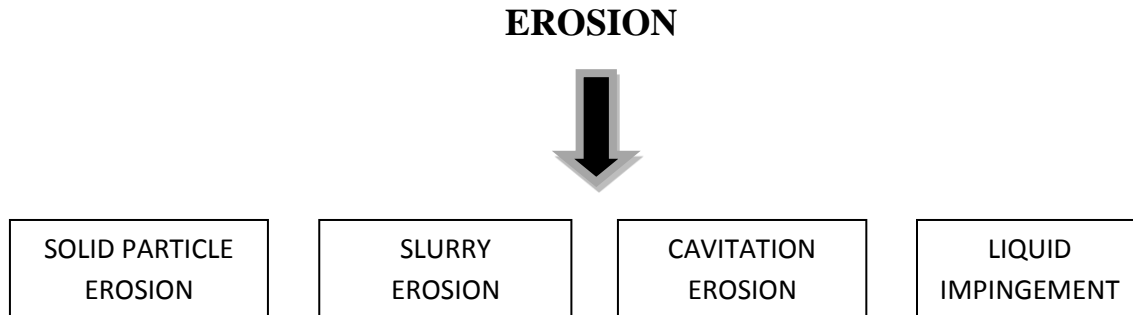


Figure 1.8: Subsurface deformation and Cracking

1.5.3 Types of Erosion wear

Erosion can be classified into various types depending upon interaction taking place between the target surface and the impacting substance.



Solid Particle Erosion (SPE)

It is the loss of material that results from repeated impact of small, solid particles entrained in air or gas. In some cases SPE is a useful phenomenon, as in sandblasting and high-speed abrasive cutting, but it is a serious problem in many engineering systems, including steam and jet turbines, pipelines and valves carrying particulate matter. Solid particle erosion is to be expected whenever hard particles are entrained in a gas medium impinging on a solid at any significant velocity (greater than 1 m/s).

Cavitation Erosion

It is defined as the repeated nucleation, growth, and violent collapse of cavities, or bubbles, in a liquid. In practice, all liquids contain gaseous, liquid, and solid impurities, which act as nucleation sites for the cavities. When the liquid that contains cavities is subsequently subjected to compressive stresses, that is, to higher hydrostatic pressure, these cavities will collapse. This collapse is directly responsible for the erosion process.

Liquid Impingement Erosion

It has been defined as “progressive loss of original material from a solid surface due to continued exposure to impacts by liquid drops or jets”. Liquid impingement erosion is related to repeated impacts or collisions between the surface being eroded and small discrete liquid bodies. The significance of the discrete impacts is that they generate impulsive contact pressures on the solid

target, far higher than those produced by steady flows thus, the endurance limit and even the yield strength of the target material can easily be exceeded, thereby causing damage by purely mechanical interaction.

Slurry Erosion

It is defined as that type of wear, or loss of mass, that is experienced by a material exposed to a stream of slurry. This erosion occurs either when the material moves at a certain velocity through the slurry or when the slurry moves past the material at a certain velocity. Slurries erode by the action of abrasive particles in the liquid which results in the failure of the surface of material in one or the other mode depending upon the conditions to which the system is exposed. Slurry erosion is a serious problem for the industries, which deals with the liquids having solid particles entrained in them. When such a mixture of liquid and solid particles termed as slurry come in contact with the machine element, the removal of material takes place from the surface making the component redundant from the surface.

1.5.4 Parameters affecting on erosion wear

The prominent parameters and their effect on erosion wear are as under:

➤ Impact angle

Impact angle is defined as the angle between the target surface and the direction striking velocity of the solid particle. The rate of mass loss due to erosion is a function of impact angle of particles. The variation of erosion wear with the impact angle is different for brittle and ductile materials. The maximum erosion occurs at 20-30 degrees impact angles for ductile materials. Whereas, the maximum erosion wear occurs at 90 degree impact angle in case of brittle materials.

➤ Velocity of solid particles

Velocity of solid particle strongly affects the erosion wear. The impact velocity has dominant effect on the material removal rate. As particle velocity increases there is significant increase in erosion rate. The erosion rate is generally related to the particle velocity using power law

relationship in which the power index for velocity varies in the range of 2-4. Gandhi et al(1999), evaluated the erosion rate is a function of velocity.

$$\text{Erosion rate} = f(\text{velocity}^{2.6}) \dots\dots\dots 1.1$$

➤ **Hardness**

Hardness is the characteristic of a solid material expressing its resistance to permanent deformation. Surface hardness as well as hardness of solid particles has profound effect on the erosion wear mechanism. Hardness ratio has been defined as the ratio of hardness of target material to the hardness of solid particles. Gandhi et al.(2008,)developed a correlation between hardness ratio of particle to metal $K_{(H_p/H_T)}$ and erosion rate i.e.

$$E_{D90} = 6.62 \times 10^{-14} \times K_{(H_p/H_T)} V^{2.02} \times d^{1.62} C_w^{-0.285} \dots\dots\dots 1.2$$

➤ **Particle size and shape**

Particle size and shape is also one of the prominent parameter, which affect erosion wear. Many investigators have considered solid particle size important to erosion. The erosion wear increases with increase in particle size according to power law relationship. The effect of particle shape on the erosion is not very well established due to difficulties in defining the different shape features. Generally roundness factor is taken into consideration. If roundness factor is one then the particles are perfectly spheres and a lower values show the particle angularity.

➤ **Solid concentration**

Concentration is amount of solid particles by weight or by volume in the fluid. As concentration of particle increases more particles strike the surface of impeller which increase the erosion rate, the concentration of slurries can vary from 2% to 50% depending upon the type of slurry. However, at very high concentrations particle interaction increases and this decreases the striking velocity of particle on the surface.

1.6 TYPES OF TEST RIG

Miller Test Apparatus

This test apparatus is designed and developed by Miller to evaluate relative abrasion wear of different material. In this test method, the wear test specimen is fixed in a sample holder attached to a reciprocating arm carrying a load of 22.24 N, which runs in a standard sand slurry. The wear sample of size 25.4mm x 12.7mm is to be tested for around six hours and its weight loss is measured in the interval of each two hours. The data obtained from this test method is used to compare the relative erosion behavior of the two materials and thus the Miller test can be used for selection of pipe material for given slurry.

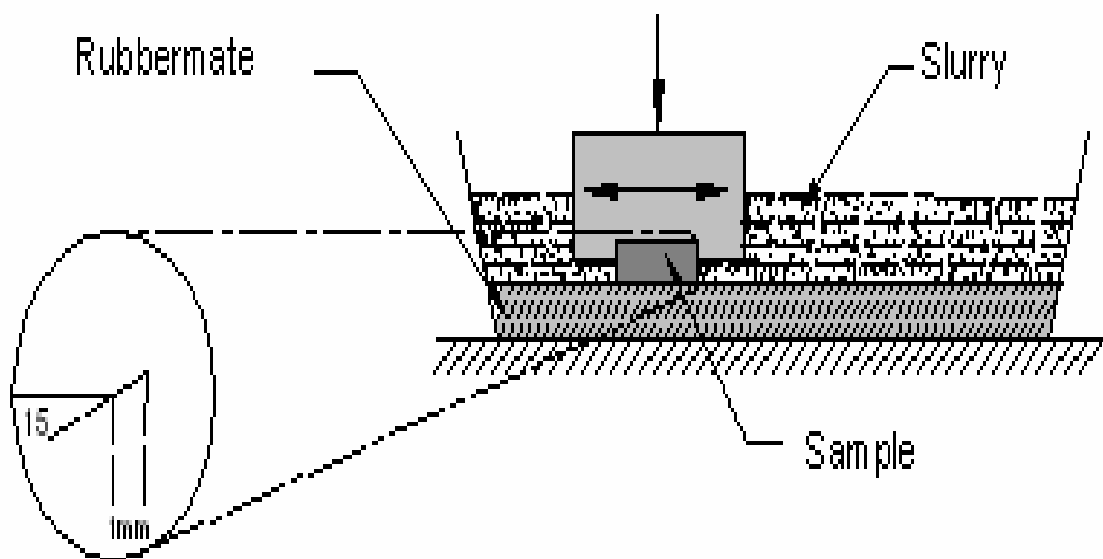


Figure 1.9: Miller Test Apparatus

Slurry Pot Tester

In this test rig, the wear specimens are rotated in a cylindrical pot containing solid-liquid mixture. This test rig is small in size, simple in design, easy to operate, economical and can be used to generate experimental data at an accelerated rate. The specimen is held in a fixture connected to a rotating steel shaft. The propeller having two blades at the end connected to a rotating shaft keeps the solid particle suspended in a liquid. The relative motion between the wear specimen and the slurry causes erosion wear. Effect of various operating parameters like concentration, velocity and impact angle can be easily calculated.

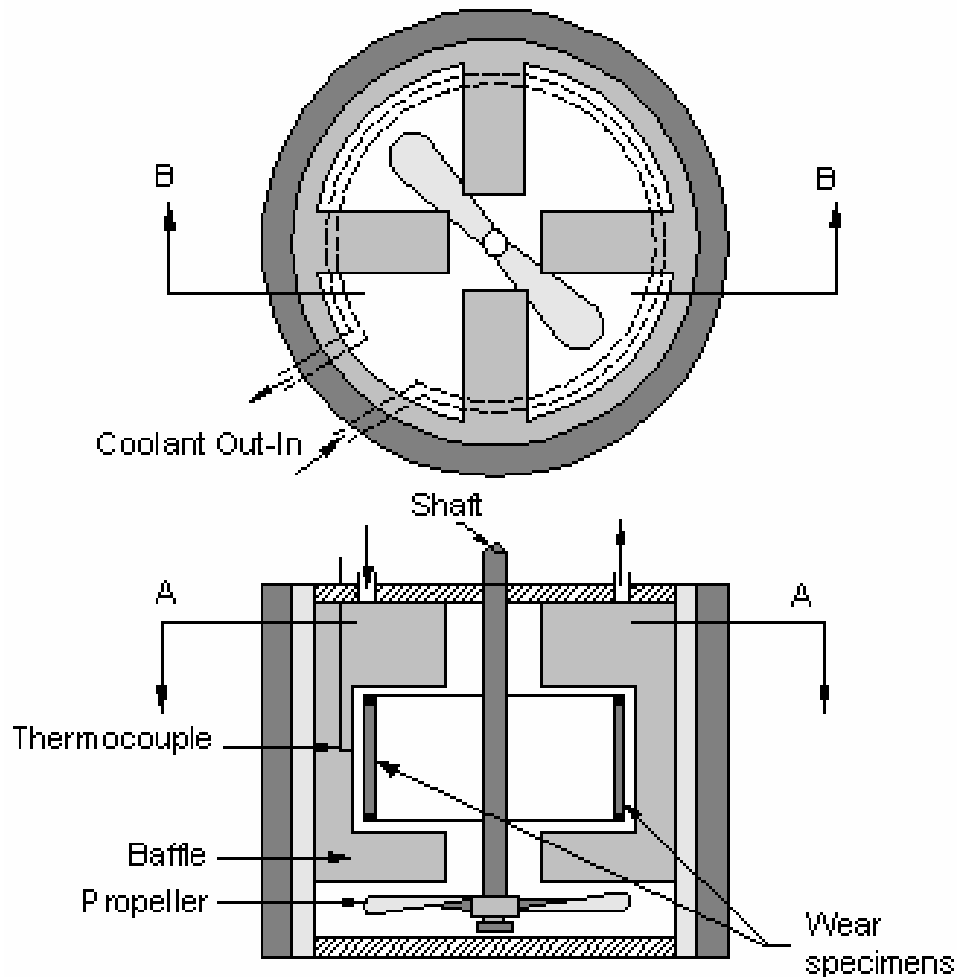


Figure 1.10: Slurry Pot Tester

Jet Impingement Tester (JIT)

In this type of test rig, a flat specimen is subjected to a jet of solid-liquid mixture as shown in Figure 1.11. The specimen can be oriented at different impact angles in the range of 0 to 90 degree. It comprises of a pump and an ejector to issue a jet through a nozzle. Jet impingement tester simulates the wear for direct impact of solid particles in equipment such as pumps, bends, tee junctions, elbows, contractions etc. This type of tester provides very good control over various parameters of erosion wear.

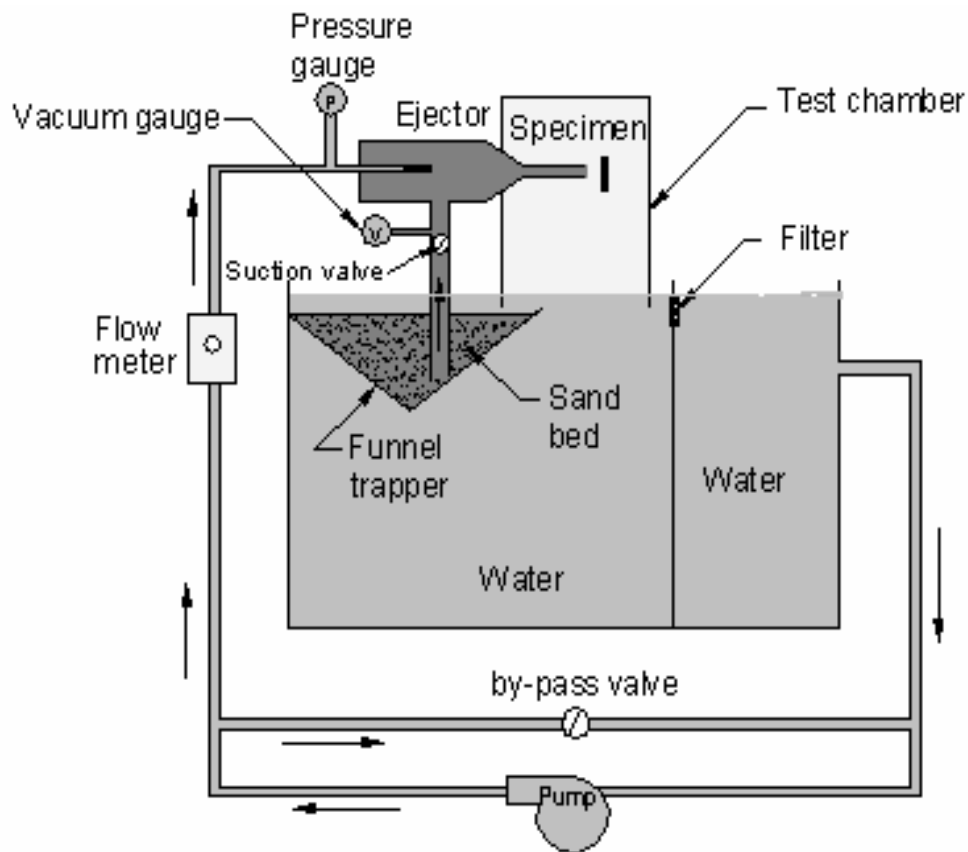


Figure 1.11: Jet Impingement Tester

Falling Jet Test Apparatus

In falling jet test apparatus, the wear specimens were rotated in a vacuum chamber and a jet of solid-liquid mixture falls on the specimen due to gravity flow. This test apparatus was designed and developed by Lin and Shao to study the effect of particle impact angle. In this test rig, four wear specimens of size 25mm x 10mm x 5mm were clamped in specimen fixtures mounted on four horizontal arms rotated by a variable speed electric motor. The radius of each arm was 104.5 mm. This assembly is kept in a vacuum chamber as shown in Figure 1.12. The slurry in the chamber falls freely under gravity from a barrel of 25 liters capacity where a stirrer is used to keep the solid-liquid mixture under suspension. The impact angle and velocity are calculated from the vector addition of the fall velocity and rotating speed of the specimens. The partial vacuum in the chamber of the specimens minimizes the spreading effect of jet, which generally occurs in jet impingement tester. However, difficulty in maintaining the partial vacuum in the chamber limits the use of this test rig.

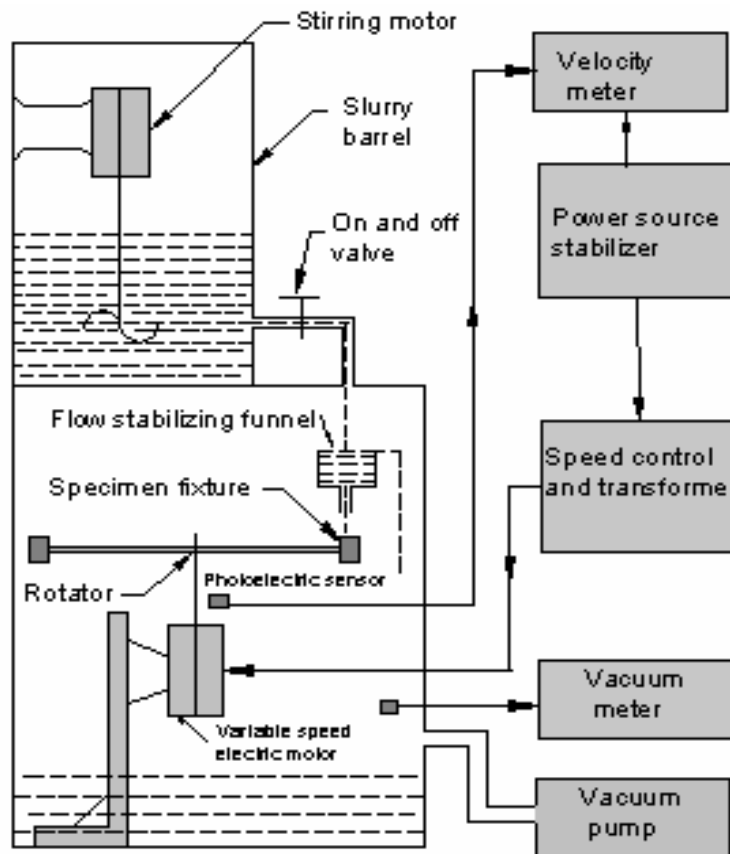


Figure 1.12: Falling Jet Test Apparatus

Jet-in-Silt Apparatus

This test rig is used to investigate the slurry erosion properties of different types of coatings. This test rig contains a transparent tank consisting of two compartments; a lower one which is smaller in diameter to store concentrated mixture and an upper one of bigger diameter to store liquid only as shown in Figure 1.13. The upper tank contains clear water which is circulated by the pump into the test section containing four test specimens subjected to uniform upward flow and remaining water is utilized to set up the fluidized bed in lower tank. The liquid jet from the nozzle, located at the center of the test section sucks up the slurry, which is mixed with the jet fluid to impinge on the test specimen and thereafter the mixture is radially exhausted through the silt between the specimen and the guide plate. The concentration of solid particles in the fluidized bed can be easily regulated, by controlling the flow rate of the liquid fed to the distributor.

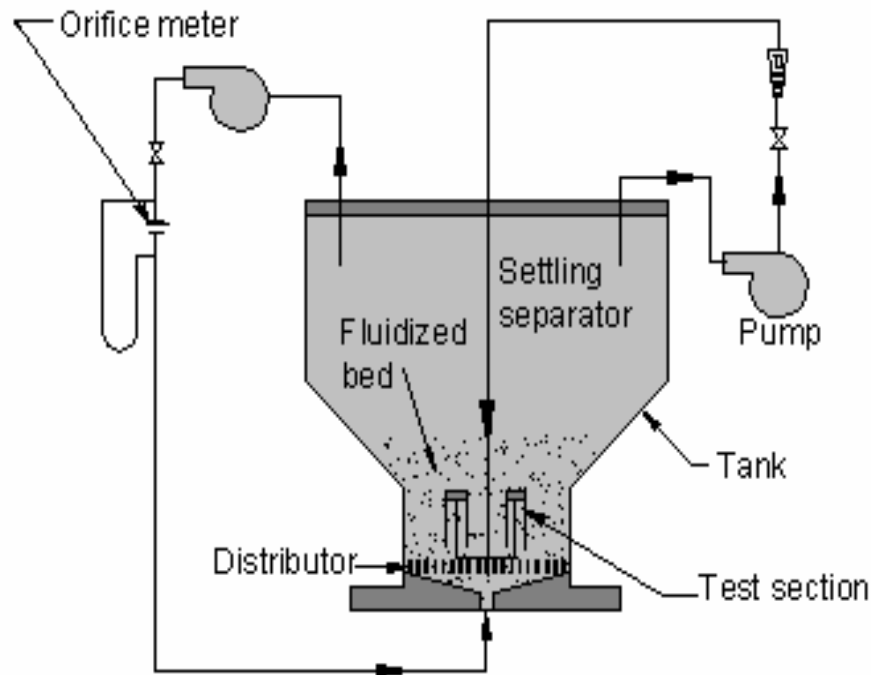


Figure 1.13: Jet-in-Silt Apparatus

Centrifugal Erosion Tester

This test rig can be used in either atmospheric condition or vacuum. The erodent particulate slurry is fed into the center of a rotor to move outwards along radial channels as shown in Figure 1.14. The slurry leaves the rotor at a speed governed by the peripheral speed of the rotor. Stationary specimens are arranged around the rim of the rotor, and the method can be used to compare the erosion behavior of different materials. This type of erosion tester is also used to evaluate the erosion rate of different materials at elevated temperature.

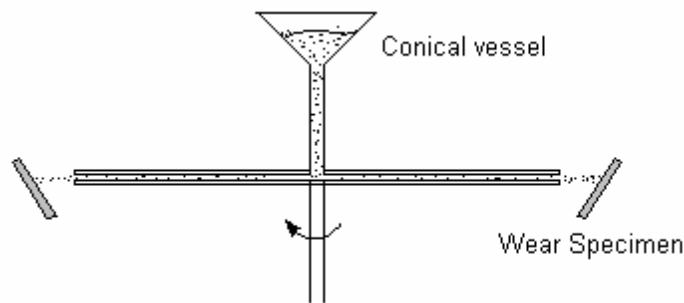


Figure 1.14: Centrifugal Erosion Tester

Coriolis Erosion Tester

In this test rig, the slurry is accelerated centrifugally from a rotating bowl through two small radial channels located at 180° apart. The wear specimens are to be fixed on the channels. The Coriolis force increases the slurry interaction with the back wall of the wear specimens.

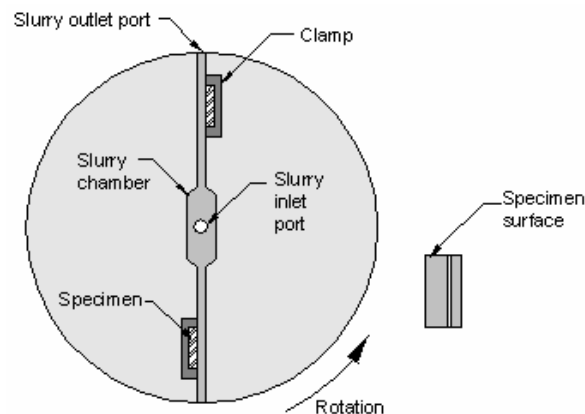


Figure 1.15: Coriolis Erosion Tester

1.7 MOTIVATION FOR THESIS WORK

Slurry erosion is a problem seen in industrial applications. For e.g., in chemical industry, refineries etc. Material loss due to erosion wear is a serious problem associated with flow of solid-liquid mixtures. Slurry erosion limits the useful life of equipment and their efficiency. Erosion is therefore a critical parameter for design, selection and operation of the hydraulic transportation system. Engineering interest is to estimate the service life of equipment / components subjected to slurry erosion and to investigate the possibilities of enhancement of their life.

CHAPTER-2

LITRATURE REVIEW

Erosion may take place due to mechanical interaction between the target surface and fluid. The erosion wear has categories as solid particle erosion, liquid impingement erosion and cavitation erosion. Solid particle erosion occurs due to direct impact of solid particles (present in slurry) on the pipelines, pumps and its components. Liquid impingement erosion is associated with the continuous impact of liquid jet on the target surface and capitation erosion is defined as the repeated nucleation, growth, and violent collapse of cavities, or bubbles, in the liquid resulting in localized removal of material from the target surface.

Many researchers have been trying to reduce the wear through various techniques but it has been difficult to find out the common cause and remedy of this problem due to its variation and dependency on large number of parameters. The parameters that affect the erosion wear in slurry transportation systems are impact velocity, impact angle, size and shape of solid particle impacting on target surface, concentration of slurry, material of target surface, and particle size distribution in the slurry, slurry viscosity and combination of all of these.

Ahmed et. al. (1983) assume that impact angle α is independent of velocity, an equation for wear of cast iron (hard and brittle) established as

$$W = 1.061 \times 10^{-8} [1 + \sin(\frac{\alpha - \alpha_1}{90 - \alpha_1} \times 180 - 90)] V^{2.3875} \quad (2.1)$$

α_1 is the angle at which wear develops and it is taken as zero for simplicity. Observations are taken at $\alpha = 60^\circ$ and 90° with different velocities. The 90° impact angle showed higher wear for any arbitrary velocity value.

Andrews and Horsfield (1983) performed the test with a jet of gas and solids particles to study the mechanics of an eroding surface. They stated that increasing the particle concentration causes a decrease in the erosion rate due to the interference of the particles themselves

Shook et al. (1990) measured the particle size distribution in a flow of sand and water in a pipe. The distribution was not homogeneous and higher particle concentrations occur in the bottom of the pipe. That is, for a fixed mean of solids concentration, as the slurry velocity increases the particle distribution becomes more uniform, which results in less wear at the bottom of pipe and more near the top and sides of a pipe.

Singh et al. (1991) found that both 304 and 316 stainless steels have the same rate of wear when impinged with an air jet containing SiC particles that were 160 microns in diameter and angular shapes. In both metals wear rate fastest when the impingement angle was at 30° and it was the slowest at 90°. This information is very useful when designing a test because it indicates where attention must be directed to evaluate the maximum wear locations. Wear measurement must not be concentrated only at a section of a flow loop where the flow makes an abrupt 90° change.

Lynn et al. (1991) have studied particles size effect on slurry erosion using a pot tester at a constant velocity of 18.7 m/s and using a relatively a dilute suspension 1.2% by weight of silica carbide in oil for different equisized diameter ranging from 20 μ to 500 μ . Tests were performed on steel specimens over a maximum period of 60 minutes. They conclude that for particles sizes greater than about 100 μ the erosion rate was proportional to the Kinetic energy dissipated by particles during impact but for particles size less than 100 μ other metal removal mechanism become increasingly significant. Both collision efficiency and impact velocity of particles decreased with decreasing particles size.

Miller and Miller (1993) have shown that erosion rate increases rapidly as the slurry concentration increases to 10% by weight, but by increasing concentration more than 20% by weight the erosion rate dependence is relatively unaffected by further increases in concentration.

Gupta et al. (1995) studied the effect of velocity, concentration and particle size on erosion wear. The experiment was performed by pot tester for two pipe materials, namely brass and mild steel. They evaluated that for a given concentration, erosion wear increases with increase in velocity and for a given velocity, erosion wear also increases with increase in concentration but

this increase is comparatively much smaller. They also concluded that erosion wear decreases with decrease in erodent particle size.

Zhong and Minemura (1995) state that cast iron and stainless steel erosion decreases with concentration of slurry. Evaluating the effects of various solid- liquid slurry flows in pumps.

Yoshiro Iwai and Kazuyuki Nambu (1997) studied the effect of concentration, velocity and impact angle on pump lining material on jet erosion tester. They formulated an empirical relation of predict the wear.

$$\text{wear} \propto (v - v_o)^n C^m (d - d_o)^3 \quad (2.2)$$

Where v_o and m are dependent on the particle size but n is number of particles.

v_o = Critical velocity

d_o = Critical diameter of solid particles

They also evaluated that rubber owes its high slurry wear resistance than other two pump lining materials (fluid elastomer, polyurethane).

R Dasgupta et al. (1998) evaluated the effect of sand slurry concentration on steel using DUCOM made TR 41 erosion tester. They also varied the rotational speed and traverse distance during the test. They concluded that increase in the concentration of sand reduces the erosion rate. They also concluded that erosion rate deteriorates with rotational speed. They were failing to clearly show the effect of traverse distance on erosion wear.

Xie et al. (1999) determined that for very dilute slurries, where the solids concentration is less than 1% by volume, or when the particle-to-particle distance is greater than 20 times a particle diameter, the effect of the solids concentration can be neglected, because the particles do not interfere with each other.

Gandhi et al. (1999) measured the erosion rate of steel plating by a jet of sand and water. The particles ranged from 200 to 900 microns and the solids concentration from 20 to 40 % by weight. Using velocities from 3 to 8 m/s they evaluated that the erosion rate = f (velocity^{2.6}).

When changing the material of the eroding surface the exponent of particle velocity also changes.

Clark et al. (1999) measured a rotational velocity and relate a slurry wear rate to an exponential function of that velocity. This rotational velocity is not a particle velocity; it is the angular velocity of a spinning disk in a Coriolis tester. That tester works by forcing slurry through two, oppositely oriented, small channels that are on a spinning disk with centrifugal force and uses the Coriolis force to direct particles towards a surface to be eroded. The particle velocity is dependent on the rotational velocity of the tester. In trying to correlate the rotational velocity to a wear rate they did not evaluate a single value for the velocity exponent and attributed the lack of a constant value to a changing environment in the slurry flow. When one parameter is changed like velocity, other parameters also changed. For instance, they specifically mentioned how the thickness of the particle bed near the eroding surface changes, which affect the velocity-wear rate relationship. They concluded that unless all other parameters are held constant, a single relationship between velocity and wear rate is difficult to obtain.

Walker and Bodkin (2000) studied the sand and water flows in pump with particle sizes from 150 to 1000 microns and impeller speeds of 18.8 and 23.4 m/s, they shown that with solids concentrations from 10 to 34% by volume the erosion rate is independent of the concentration.

Abbade and Crnkovic (2000) found that changing the surface hardness did not significantly affect the wear rate. They used a low carbon, niobium-titanium, steel (API 5L X65) in annealed and heat treated conditions, which doubled the metal's yield and tensile strengths. Against this metal they directed a jet of slurry at 4.5 m/s, which was made of water that contained 3 5 by weight of sand with particles size from 150 to 300 microns. The fastest wear occurred at an angle of 30° and it was slowest at 90°, which implied a ductile-type wear, but both the heat-treated and non-heated surfaces displayed the same wear rate, for the same particle direction.

Hawthorne H.M. et al (2001) has conducted Coriolis tests for the evaluation of slurry erosion on different materials. Slurries consisting of glass beads of size 90- 200 micron size with 10% slurry concentration were taken and tests were performed on 1020 steel and copper at different impingement angles of 90-20 degrees. It was also observed that in slurry jet testing, most particles impact the specimen above its critical velocity resulting severe plastic deformation. In contrast, in the Coriolis test most particle impacts result in only elastic deformation or mild plastic deformation. Hence, elastic as well as plastic properties of specimen materials affect their performance in a Coriolis slurry erosion evaluation, thus the results obtained from Coriolis tests were more accurate.

Clark et al. (2002) has studied the effect of Particle velocity and particle size in slurry erosion. The various factors which affect the slurry erosion such are concentration of particles, particle impact speed, particle impact angle, particle size, particle density, hardness, nature of suspending liquid, nature of slurry flow (esp. local turbulence), nature of material. The loss of material must be measured by changes in surface profile rather than mass loss.

Ghanta et al. (2002) suggested two different solids namely coal and copper ore having different surface characteristics. They observed that coarse size coal-in-water slurries exhibit lower viscosities compared to fine size coal-in-water slurries, whereas due to its opposite surface characteristics, copper or coal behaves in a reverse way. The results have also shown that PSD has market influence on viscosity of suspension. For coal water system 60:40 weight proportion gave maximum reduction and for copper ore-water system 40:60 gave maximum reduction. From this it reveals that mixing fines particles with coarse slurry could reduce the viscosity of the suspension.

Wood R.J.K. et al (2004) has covered research that has been aimed at determining the distribution of erosion rates and the erosion mechanisms that occur over wetted surfaces within pilot scale pipe systems handling water-sand mixtures at 10% by volume concentrations and at a mean fluid velocity of approximately 3 m/s. The wall wear rates, obtained by gravimetric measurements, as a function of time are discussed. The erosion rates, expressed as volume loss

per impact (determined gravimetrically and via computer models) in bends are found to agree well with simple laboratory scale water-sand jet impingement tests on planar stainless steel samples.

Gandhi et al. (2004) has conducted experiments in a pot tester for analyzing the effect of orientation of plane surface relative to its motion in solid-liquid suspensions. They conducted experiments at various operating conditions by varying the impact angle, Flat brass test pieces flush with a surface of hardened carbon steel plate (hardness= RC45) were taken. The orientation or impact angle was varied from 0° to 90° and concentration range was 20-40% by weight . It has been found that the erosion wear decreases with increase in orientation angle but this decrease was not consistent. It was seen that wear increases with the increase in orientation angle till 30° and then decreases with increase in orientation angle up to 90° for various range of velocities and particle sizes. Further it has been concluded that wear at 30° angle was 3-4.5 times higher than at 90° orientation angle and also wear increases with increase in velocity and particle size but decreases with increase in solid concentration under different impact angles.

Neville et al. (2005) studied the erosion-corrosion behavior of WC-Metal matrix composites (EFM, EFW, EGC, EGG). The materials were eroded by two sizes of silica sand with stream velocities of 10 and 17 m/s at 65 °C. Test was conducted by varying the concentration. They evaluated that WC grain size fractions has very little effect on wear. They also concluded that the erosion–corrosion rate is strongly dependent upon erodent size, impinging velocity and solid loading.

Tian Harry H. et al (2005) have observed the erosive wear of some metallic materials such as high chromium white iron and aluminium alloy using Coriolis wear testing approach. In the present study, the correlation between wear rate and particle size on the tested materials is discussed. Factors, which should be considered in wear modeling and prediction, have also been addressed. They have studied that the larger solids particles resulted in higher mass loss in all test materials. Although the wear rates at smaller particle sizes were relatively close within each material group, the wear rate difference was significantly widened with larger particle sizes.

Berget et al. (2007) evaluated the effect of grain size distribution on erosion wear. WC-Co-Cr powder was coated on to 22Cr5Ni steel. Three different ranges of grain size (15-45, 25-38 and 36-45 μm) were examined with jet erosion tester. Silica particles of 250 μm at 0.25% concentration, impinges on specimen at velocity of 14m/s and 23m/s. They evaluated that with increase in grain size of powder erosion reduced substantially. Erosion wear of 36-45 μm is almost 1/4th as compared to 15-45 μm .

T. Manisekaran et al. (2007) studied the effect of surface treatment on erosion rate of 13Cr 4Ni steel at various angles of impingement. Pulsed plasma nitriding and laser hardening techniques were used for surface hardening. The results have shown that Laser hardening process has good performance at all angles of impingement due to martensitic transformation of retained austenite. They also concluded that by increasing erodent particle size erosion rate also increases.

M.A. Al-Bukhaiti et al. (2007) studied the influence of impingement angle on erosion mechanisms of 1017 steel and high-Cr white cast iron using a slurry whirling-arm test rig. They found that by changing the impact angle the mechanism of erosion also changes. At low impingement angles, ploughing and micro cutting were the predominant erosion mechanisms of material removal. Whereas, at high impingement angles plastic indentation was the main reason for erosion mechanisms.

Williams A. John et al (2007) proposed that when material is lost from loaded surface either entirely or principally through some form of mechanical interaction the concentration, size and shape of the debris particles carry important information about the state of the surfaces from which they were generated and thus, by implication, the potential life of the contact and of the equipment of which this forms part. To use debris examination as a diagnostic aid in assessing health of the operating plant, which may contain many tribological contacts, requires not only careful and standardized procedures for debris extraction and observation but also an appreciation of the mechanism by which wear occurs and the regimes in which each of the contacts of interests operates when displayed on an appropriate operational map.

B K Gandhi et al. (2008) evaluated the erosion wear of ductile material under normal impact conditions. By keeping solid concentration as 10 % wt, velocity as 3m/s and particle size as 550_μm test was conducted on seven different materials. Those were aluminium alloy (AA6063), copper, brass, mild steel, AISI 304L stainless steel, AISI 316L stainless steel, and turbine blade steel. Solid particles of slurry were mixture of quartz, alumina and silicon carbide. They evaluated that erosion of target material is dependent on ratio of hardness of solid particles to hardness of target material and independent of hardness of target material and hardness of slurry particles. By varying particle size, concentration and velocities they formulated an empirical formula for erosion rate at normal condition:

$$E_{D90} = 6.62 \times 10^{-14} \times K_{(H_p/H_T)} V^{2.02} \times d^{1.62} C_w^{-0.285} \quad (2.3)$$

Where V= velocity of impacting particle

d= particle size

C_w =Concentration by wt

$k_{(H_p/H_T)}$ = constant, value depends on hardness of target material and of particles.

S.C. Mishra et al. (2009) studied all the parameters affecting the erosion wear using jet erosion tester on fly ash-quartz coating. By varying different parameters they evaluated that impact angle is the most significant factor influencing the erosion wear of fly ash-quartz coating. They also evaluated that maximum erosion takes place at impact angle of 90°.

B K Gandhi et al. (2009) studied the effect of particle size on erosion wear of aluminum alloy (AA6063) using pot tester. Quartz particle were used as slurry of eight different sizes varying between 37.5 and 655_μm. keeping the concentration of 20% by weight and velocity as 3m/s experiment was conducted. They found that the erosion wear increases with increase in mean particle size.

Tian et al. (2009) evaluated erosion wear rate using coriolis erosion pot tester of three high-chromium white iron alloys containing 25%, 30% and 40% of chromium. They have taken three particle size range of silica sand with 10 micron, 148 micron and 660 micron with clean water at varied temperature range of 32°C and 47.5°C and also evaluate the corrosion wear of same material by using silica sand water slurry with addition of sulphuric acid (H_2SO_4), and sodium chloride (NaCl). They found that with increase of practical size erosion wear rate also increases and temp rise play important role with corrosion wear.

Huang et al. (2010) developed a single particle erosion model and developed a comprehensive phenomenological model for erosion of material in slurry pipeline flow based on the turbulent flow theory and his previous model. This model captures the effects of particle shape, particle size, slurry mean velocity, pipe diameter, fluid viscosity and the properties of target material. This model shows that erosion rate has a power-law relation with particle shape and size, slurry mean velocity, liquid viscosity and pipe diameter. Huang formulated the equation written below:

$$ER = b^{1.375} \times c^* \rho_p^{1.1875} d^{0.5} u_o^{3.375} \gamma^{0.516} R_{ed}^{-0.6875m} \quad (2.3)$$

Where b and c* are constants. Their value depends on properties of target material.

ρ_p = Particle density,

d = Pipe diameter,

u_o = Slurry mean velocity,

R_{ed} = Reynolds Number in S.I. units.

Taking logarithms of both sides of the above equation and using the method of least squares, we got the best values of b and c* to be 0.072 and 0.148, respectively.

Erosion rate with pipe diameter and liquid viscosity has a weak relation, namely, erosion rate slightly decreases as the pipe diameter increases; while the impact of liquid viscosity on erosion rate depends on the erosion location on the periphery of a pipe.

CHAPTER 3

EXPERIMENTAL SETUP

Material loss due to erosion wear is a serious problem associated with flow of solid-liquid mixtures. Slurry erosion limits the useful life of equipment and is therefore a critical parameter for design, selection and operation of the hydraulic transportation system. Engineering interest is to estimate the service life of equipment / components subjected to slurry erosion and to investigate the possibilities of enhancement of their life. A number of bench scale test rigs are available to evaluate the slurry erosion. Among the various selected test rigs, a jet erosion tester has been commonly used by several investigators. Other reason for the selection of jet type of test rig compared to other rotating equipment and its advantages:

- The erosion of material with different impingement angles is possible.
- Control of variable like velocity and concentration is easy and several test points are possible.
- Very high velocities can be achieved compared to other available test rigs.

Experimental erosion wear of the different materials are evaluated with Jet type erosion tester at Baba Banda Singh Bahadur Engineering College, Fatehgarh Sahib.

3.1 DESCRIPTION OF JET EROSION TESTER

The test rig consists of a centrifugal pump, conical tank, nozzle, specimen holder, valves and flow meter. Electric motor of 7.5 HP is used to drive Centrifugal pump has a capacity of max pressure 13.5 bar at a discharge of 240 L/min. Slurry available in conical tank as can be seen in Figure. 3.2, is sucked through a 100mm GI pipe with help of pump and delivered to the nozzle through 25 mm pipe having control valves and electromagnetic flow meter located upstream. Slurry is re-circulated during test. The main valve and bypass regulator valve between delivery side and nozzle is used to control the flow rate of the slurry. The rectangular tapered tank having 650×650 mm at top which converges to 100×100 mm at the bottom through a length of 700mm was used to store the slurry. A mesh is provided in the bottom of the tank to avoid the object from falling into the tank and get struck inside the pipeline.

Slurry flowing through the pump at high pressure is converted into high velocity stream while passing through the converging section of the 125mm long nozzle having diameter of 8 mm. the standoff distance between the nozzle and specimen can be varied from 25mm to 90mm. After striking the specimen slurry falls back into the tank. The electronic magnetic flow meter (Elmag-200M) arranged in between control valves and nozzle is equipped with digital display and contains PTEF coated liner through which the slurry flows and discharge is calculated, when a conductive fluid passes through magnetic field (applied) a voltage is induced in an electrically conductive body which is proportional to the mean flow velocity according to Faraday's law of induction.

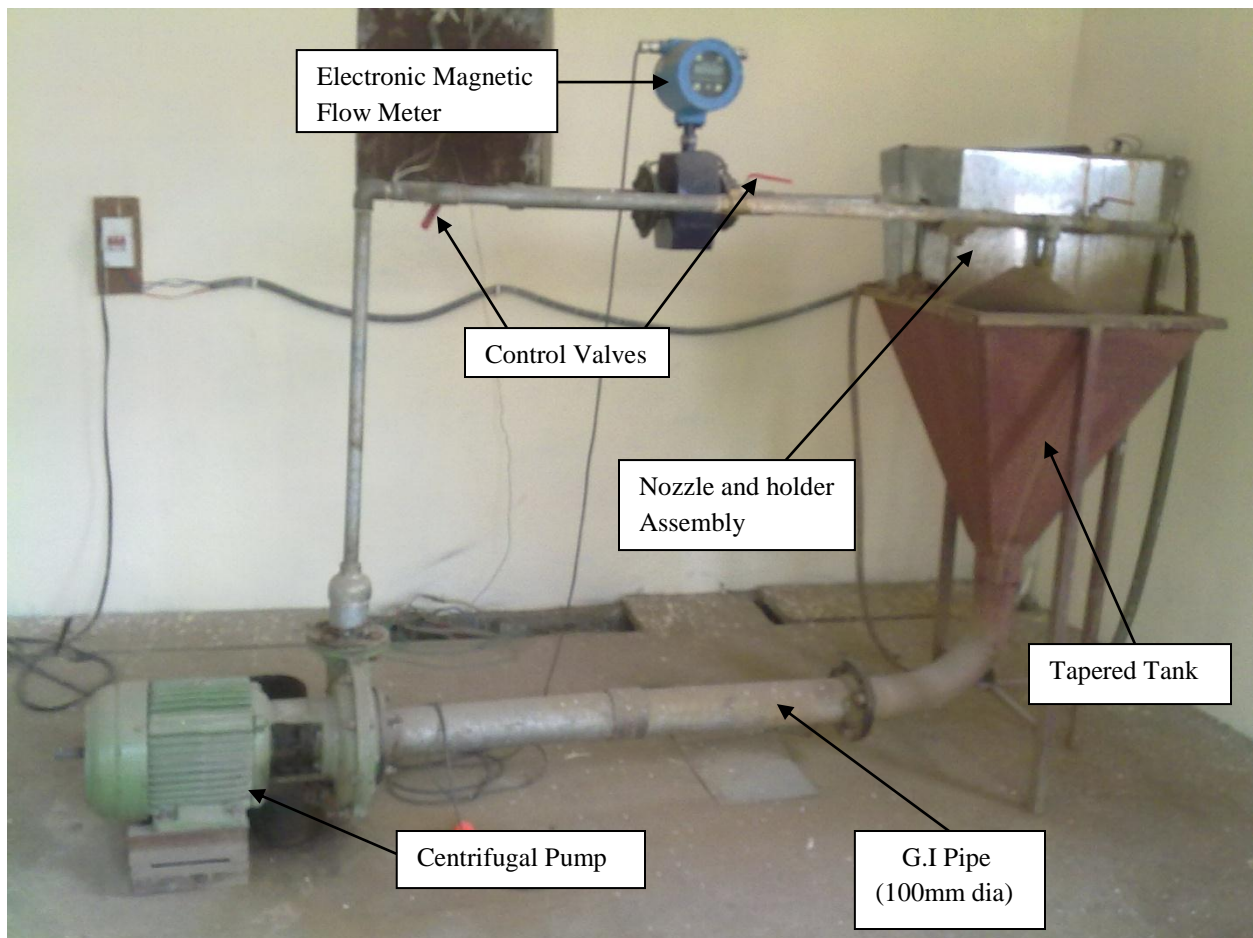


Figure 3.1: Jet Erosion Tester

3.2 WORKING OF JET EROSION TESTER

In jet erosion testing a high velocity jet strikes a flat specimen at some adjustable angle. The amount of material removed is determined by the weight loss. The material which accumulates on the specimen surface interferes with the incoming particle. The weight loss of the specimen corresponds to the average erosion over the surface.

Jet erosion tester investigate the effect of different parameters particularly the impact angle. A jet of solid–liquid mixture strikes the specimen fixed in a fixture, which can be changed at any angle with respect to the former. The pump supplies water at high pressure and the solid particles are being sucked through an injector. The slurry is mixed in the mixing chamber before the jet comes out through a nozzle.

3.3 PROCEDURE OF EVOLUTION OF DIFFERENT MATERIALS

The procedure has to be followed on erosion tester to calculate the erosion wear of different materials is as follow:

1. Firstly the specimen is cleaned properly.
2. Drying, if required.
3. Weighing the specimen (initial weight).
4. Clamp the specimen in fixture provided in test rig.
5. Setting the holder at required angle.
6. Weight the required sand as per concentration of slurry.
7. Mixing the proper amount of water and sand in tank.
8. Start the pump.
9. Adjust the flow rate to obtain desired value of mass flow rate and running the test for required time interval.
10. Removing the specimen from the fixture.
11. Cleaning and drying the specimen.
12. Weighing the specimen after erosion to measure the mass loss.
13. Repeat the steps from 4 to 13 as per requirement.

3.4 MATERIALS USED

The materials 16Cr-5Ni stainless, 13Cr-4Ni stainless steel, Grey Cast iron, mild steel are selected for parametric study of the erosion wear rate with different parameters velocity, impact angle. The properties and chemical composition of the materials are given in table 3.1. These materials are commonly used for manufacturing of pumps, turbines components and pipes

Table 3.1 Mechanical properties of different materials

Composition	Tensile strength (MPa)	Yield strength (MPa)	% Elongation	Nature
16Cr, 5Ni, .05C, 1.5Mo	880	600	21	Hard and Ductile
13Cr, 4Ni, .04C, 4Mo	823	686	23	Hard and Ductile
Mild Steel (0.1C, 0.8Mn, 0.04S, 0.04Ph)	440	370	15	Ductile
Grey Cast Iron (3.4C, 1.8Si, 0.5Mn)	172	227	5	Ductile

Chemical composition The chemical composition of mild steel, grey cast iron, 16Cr-5Ni stainless steel and 13Cr-4Ni stainless steel samples were determined by the spectrometer analysis as shown in Figure below



Figure 3.2: spectrometer

Analysis												
Start	New	Print	Del	Store	Recal	Mode	Load	Change	R&D	Exit		
Sample:												
Element	Burn 1	Burn 2	Burn 3	Burn 4	Burn 5	Burn 6	Burn 7	Burn 8	Burn 9	Burn 10	Burn 11	Average
Fe %	99.2	99.2										99.2
C %	0.0897	0.0893										0.0895
Si %	0.163	0.171										0.167
Mn %	0.410	0.402										0.406
P %	H 0.0898	H 0.0806										H 0.0852
S %	0.0276	0.0261										0.0278
Cr %	< 0.0030	< 0.0030										< 0.0030
Mo %	< 0.0050	< 0.0050										< 0.0050
Ni %	< 0.0050	< 0.0050										< 0.0050
Al %	< 0.0010	< 0.0010										< 0.0010
Co %	0.0031	0.0031										0.0031
Cu %	0.0028	0.0034										0.0031
Nb %	0.0037	0.0042										0.0039
Ti %	< 0.0020	< 0.0020										< 0.0020
V %	< 0.0020	< 0.0020										< 0.0020
W %	< 0.0150	< 0.0150										< 0.0150
Pb %	< 0.0250	< 0.0250										< 0.0250
Sn %	< 0.0020	< 0.0020										< 0.0020

Figure 3.3: Composition of mild steel by spectrometer

Analysis												
Start	New	Print	Del	Store	Recal	Mode	Load	Change	R&D	Exit		
Sample: dalbir												
Element	Burn 1	Burn 2	Burn 3	Burn 4	Burn 5	Burn 6	Burn 7	Burn 8	Burn 9	Burn 10	Burn 11	Average
Fe %	90.6											90.6
C %	3.73											3.73
Si %	1.58											1.58
Mn %	0.606											0.606
P %	> 0.800											> 0.800
S %	> 0.140											> 0.140
Cr %	0.0540											0.0540
Mo %	0.0659											0.0659
Ni %	0.230											0.230
Al %	0.0317											0.0317
Co %	0.0057											0.0057
Cu %	0.0857											0.0857
Mg %	0.0249											0.0249
Nb %	0.0427											0.0427
Ti %	0.0879											0.0879
V %	0.0303											0.0303
Pb %	> 0.250											> 0.250
Sn %	0.0219											0.0219

Figure 3.4: Composition of grey cast iron by spectrometer

Analysis												
Start	New	Print	Del	Store	Recal	Mode	Load	Change	R&D	Exit		
Sample: aseem2												
Element	Burn 1	Burn 2	Burn 3	Burn 4	Burn 5	Burn 6	Burn 7	Burn 8	Burn 9	Burn 10	Burn 11	Average
Fe %	78.7	76.6										76.7
C %	0.0505	0.0277										0.0391
Si %	0.267	0.261										0.264
Mn %	0.642	0.638										0.640
P %	< 0.0030	< 0.0030										< 0.0030
S %	< 0.0050	< 0.0050										< 0.0050
Cr %	13.5	15.8										15.6
Mo %	0.664	0.651										0.657
Ni %	4.81	5.69										5.75
Al %	< 0.0010	< 0.0010										< 0.0010
Co %	0.0674	0.0692										0.0683
Cu %	0.135	0.140										0.138
Nb %	< 0.0020	< 0.0020										< 0.0020
Ti %	< 0.0020	< 0.0020										< 0.0020
V %	0.0328	0.0395										0.0361
W %	< 0.0200	< 0.0200										< 0.0200

Figure 3.5: Chemical composition of 13/4 steel by spectrometer

Analysis												
Start	New	Print	Del	Store	Recal	Mode	Load	Change	R&D	Exit		
Sample: aseem2												
Element	Burn 1	Burn 2	Burn 3	Burn 4	Burn 5	Burn 6	Burn 7	Burn 8	Burn 9	Burn 10	Burn 11	Average
Fe %	76.7	76.6										76.7
C %	0.0505	0.0277										0.0391
Si %	0.267	0.261										0.264
Mn %	0.642	0.638										0.640
P %	< 0.0030	< 0.0030										< 0.0030
S %	< 0.0050	< 0.0050										< 0.0050
Cr %	15.5	15.8										15.6
Mo %	0.664	0.651										0.657
Ni %	5.81	5.69										5.75
Al %	< 0.0010	< 0.0010										< 0.0010
Co %	0.0674	0.0692										0.0683
Cu %	0.135	0.140										0.138
Nb %	< 0.0020	< 0.0020										< 0.0020
Ti %	< 0.0020	< 0.0020										< 0.0020
V %	0.0328	0.0395										0.0361
W %	< 0.0200	< 0.0200										< 0.0200

Figure 3.6: Composition of 16/5 steel by spectrometer

CHAPTER 4

PROPERTIES OF BOTTOM ASH

4.1 BENCH SCALE TEST

The material required for testing purpose was collected from Guru Govind Singh thermal power plant, Ropar, Punjab. Various bench scale tests were carried out on ash collected to determine the specific gravity, particle size distribution (PSD) of the solid materials. The pH value & static settling characteristics of bottom ash was determined in the laboratory at IIT Roorkee. A brief description of these tests is presented here.

4.1.1 Particle Size Distribution

The variation in the size of the particles in the solid sample and the percentage of particles present in different pre-selected size ranges are determined to establish the particle size distribution (PSD). Two methods namely sieve analysis and hydrometer analysis, can be employed to get this distribution. In the present study a known weight of sample of solid particles is taken and washed over a B.S. 200 mesh (75 μ m). Particulate materials are dried in an oven. The dried material is sieved through a set of standard sieves. Special care is taken to ensure that the sample is properly dried. The sample retained on each sieve is collected and the percentage retained on each sieve is calculated using the standard procedure.

4.1.2. Specific gravity

In the present study, the specific gravity of solid particles is determined using fixed volume bottle. In this method first take 50 ml fix volume bottle and clean it thoroughly, keep it in the oven in order to remove moisture from bottle. After 2 hours, take out the bottle from an oven and allow it to cool down, and then take the weight of bottle (W_b). After weight put some solids (over dried) about 30 grams in it and weight it again and note down this weight (W_{bs}). After this slowly pour water (distilled) in the bottle so that no air is entrapped in it and shake it well, and keep on pouring the water. Shake it well each time till all the solid get wet. Fill $3/4^{\text{th}}$ of bottle with water and put the thumb on the mouth of the bottle and shake it well for 5 minutes. Keep it for at least 2 Hours, so that air bubbles get out from the bottle. Then fill the bottle of water and

cork it. Clean it with cloth/tissue paper and weight it. Note down the weight (W_{bsw}). Now remove the solids from the bottle and clean it, Thoroughly, Dry it and fill it with distilled water. Note down the weight (W_{bw}). Calculate the specific gravity of solids as given below.

$$\text{Specific Gravity of solids} = \frac{(W_{bs} - W_b)}{\{W_{bw} - W_{bsw} + (W_{bs} - W_b)\}}$$

Where, W_b = Weight of beaker

W_{bs} = Weight of beaker and solid

W_{bw} = Weight of beaker and water

W_{bsw} = weight of beaker, solid and water

4.1.3 Static Settled Concentration

The static settled concentration is an important parameter as it decides the highest limit of solid concentration, which can be achieved by gravitational settling. The static settled concentration depends on a large number of parameters like specific gravity, shape and size distribution of solids, density and viscosity, of carrier fluid etc. It is well accepted that the optimum concentration for solids transportation is around 5 to 10% lower than the static settled value.

In the present study, the static settled concentration has been determined by preparing a slurry sample of intermediate concentration i.e. 20% (by weight) and allowing it to settle in a graduated measuring jar till the level of the solids become constant. This value of solid concentration in the settled portion of slurry is the static settled concentration. The slurry level at regular intervals of time was also recorded during the process of settling of the slurry to determine the setting rate of the slurry.

4.1.4 pH value

A pH meter was used for measurement of the pH value of the slurry of any given solid concentration. The electrode of the meter was first moistened with tap water and then calibrated with a buffer solution of a known pH value. It is cleaned by rinsing vigorously with distilled

water and then immersed in the slurry sample whose pH value was to be determined. The pH suspension was read on the digital display unit when equilibrium value was reached.

4.1.5 Rheological Behavior of Solid-Liquid Mixture

Rheological behavior of the slurry at various concentrations and flow conditions is one of the most important input data required to design of the slurry transportation system. The rheological characteristics of slurry depends on several parameters such as shape, size particle size distribution, solids concentration, carrier fluid properties etc.

Preparation of the slurry sample: For rheological test 100 ml of the ash-water suspension is prepared by mixing the required quantity of ash with distilled water. The ash was accurately weighed in an electronic type single pan balance. The suspension was mixed gently by a glass rod taking care to avoid attrition of the particles.

Rheometer: The standard Rheolab Q-C is used to calculate the rheological characteristics of the slurries which is shown in Figure 4.1. Co-axial concentric cylinder cup and bob geometry is used for measuring the rheological properties of fly ash. The bob and cup assembly is fixing using a locking device and slurry mixture is added into cup (cylinder) up to the particular mark before test. The shear stress value and viscosity measured at the shear rate range from $50\text{-}225\text{ s}^{-1}$ at the constant temperature condition $26\text{ }^{\circ}\text{C}$ with wide range of concentrations varying from 0 to 40% (by weight) for ash and water slurries.



Figure 4.1: Rheometer (Anton Paar, Germany)

4.2 PHYSICAL PROPERTIES OF BOTTOM ASH

Physical properties of bottom ash are given in table 4.1. The specific gravity of bottom ash was determined as 2.25. Particle size distribution of bottom ash given in Table 4.1 shows that the largest particle is 2000 μm and only 3% particles are finer than 75 μm . Figure. 4.2 shows the Particle size distribution of fly ash sample. Figure. 4.3 shows the static settled of bottom ash sample is 49.1% by weight. The pH values of bottom ash at various concentrations in the range of 0 to 50% (by weight) varies in the range of 7.62 to 7.75 which also represent that the sample of bottom ash is also non-reactive nature.

- (1) Specific gravity of Bottom Ash: **2.25**, particle size $d_{50} = 230 \mu\text{m}$, $d_{wn} = 162.139 \mu\text{m}$
- (2) Rheological Properties of bottom ash at temperature 26°C

Table 4.1: Rheological Properties of bottom ash

Concentration (Cw) %	Yield stress (Pascal)	Slurry viscosity(cP)	Water viscosity(cP)	Relative viscosity	Flow behaviour
0	0	---	0.995	1	Newtonian
10	0	1.01	0.995	1.02	Newtonian
20	0	1.6	0.995	1.61	Newtonian
30	0	2.2	0.995	2.21	Newtonian
40	0	4.3	0.995	4.31	Newtonian
50	0	5.6	0.995	5.62	Newtonian

- (3) pH value of slurry

Table 4.2: pH value of slurry

C_w, %	0	20	25	30	35	40	45	50
pH	7.75	7.67	7.66	7.66	7.64	7.63	7.62	7.62

- (4) Static settled concentration of slurry = 49.1 % with Initial concentration= 20% (by weight)

Table 4.3: Settled concentration of bottom ash sample

Sr. No.	Time(Minute)	Conc. (%C_w)
1	0	20
2	1	28.12
3	2	33.16
4	3	42.37
5	4	45.25
6	5	47.39
7	15	47.39
8	30	47.39
9	60	48.54
10	120	48.54
11	180	48.54
12	240	49.01
13	480	49.01

- (5) Particle size distribution

Table 4.4: Particle size distribution

Sr. No.	Particle size, μ	% finer
1	below 2000	100
2	1400	89.5
3	710	85.5
4	355	72.6
5	300	65
6	250	58.8
7	212	46.8
8	180	44.1
9	150	20.6
10	125	17.4
11	90	13.5
12	75	3

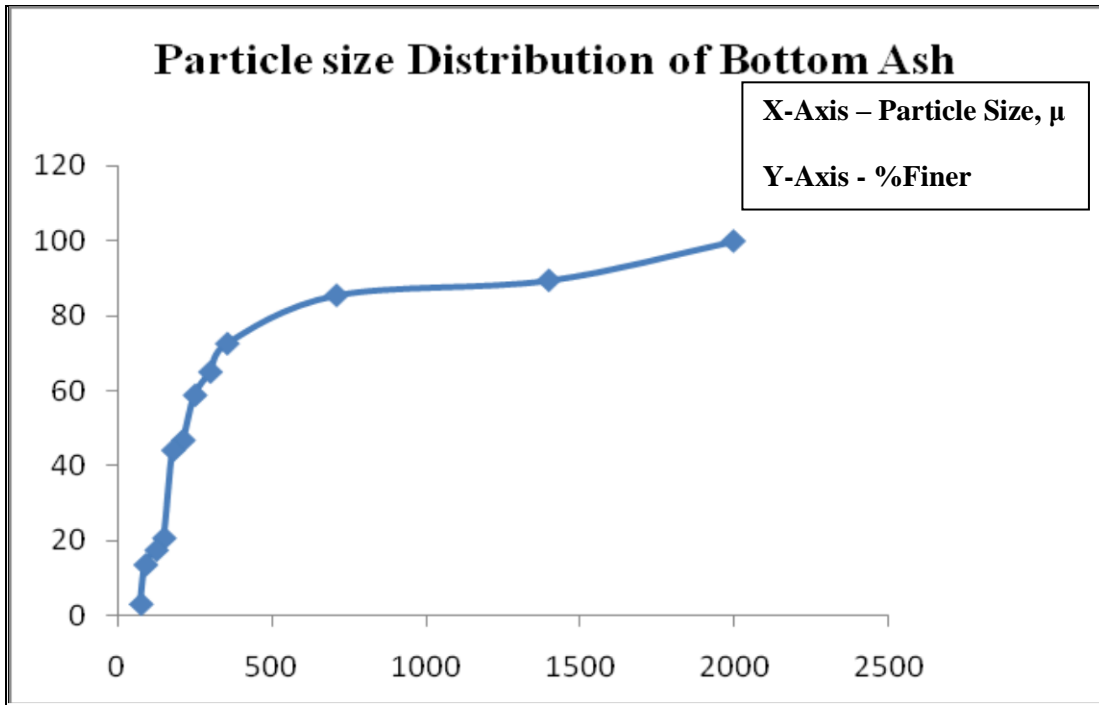


Figure 4.2: Particle size distribution curve of bottom ash sample

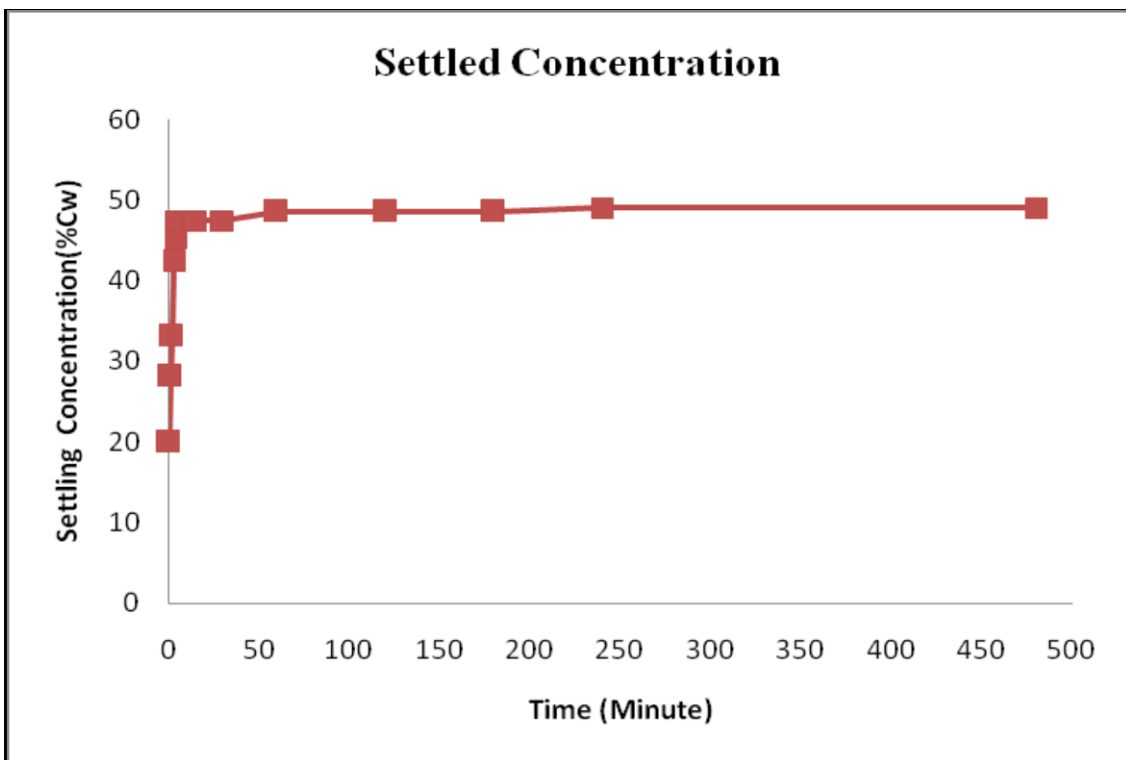
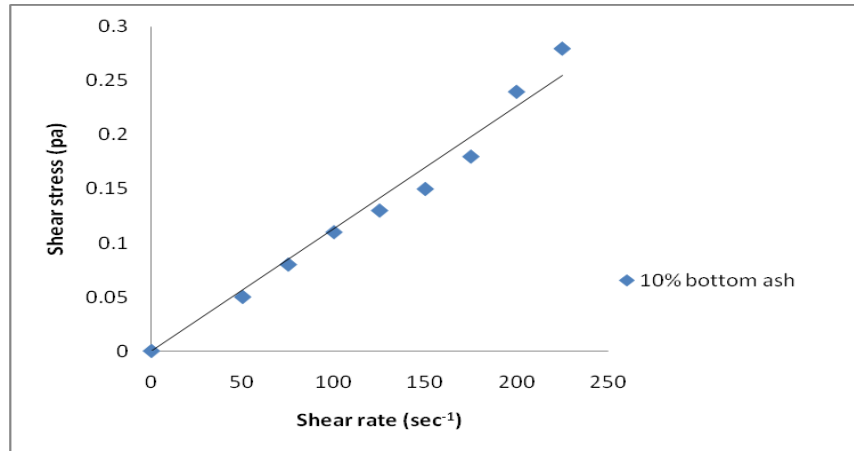


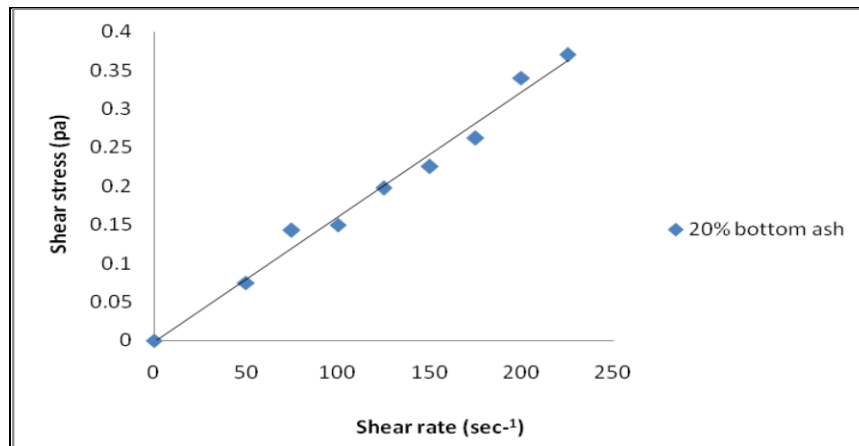
Figure 4.3: Settled concentration curve of bottom ash sample

Graphical representation of the Rheology of bottom ash slurry sample with variation of concentration

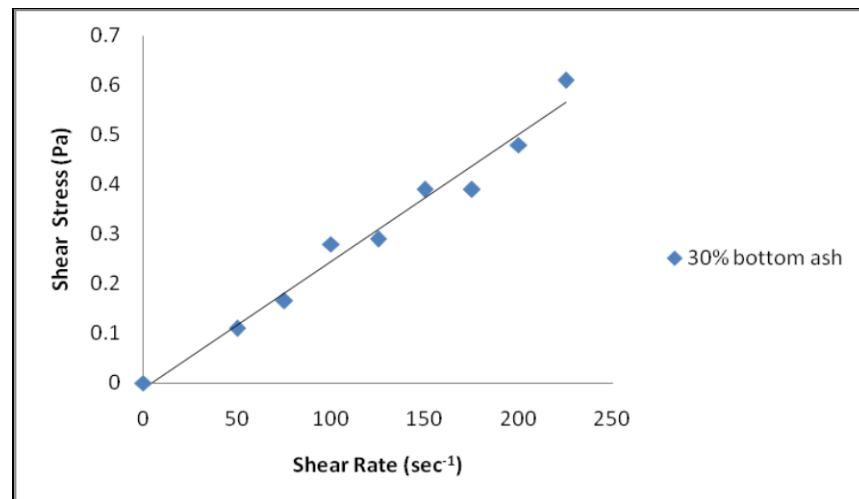
(a)



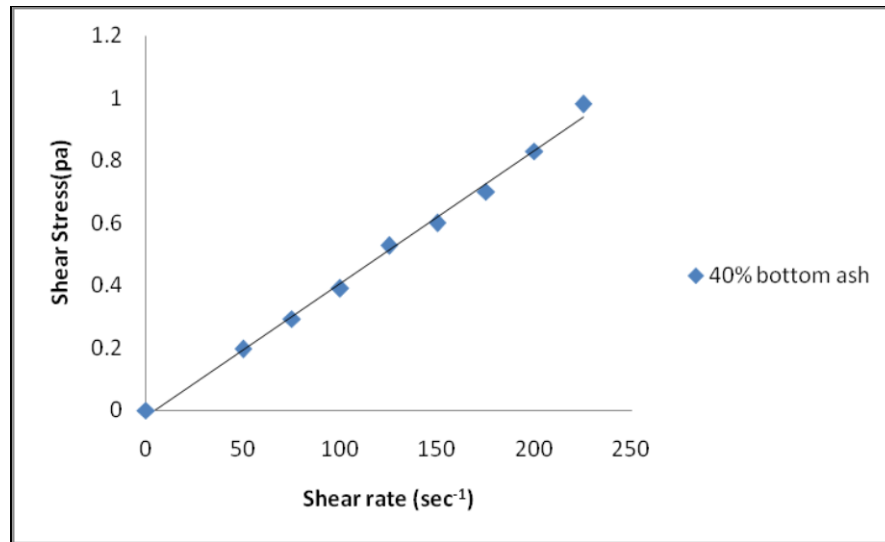
(b)



(c)



(d)



(e)

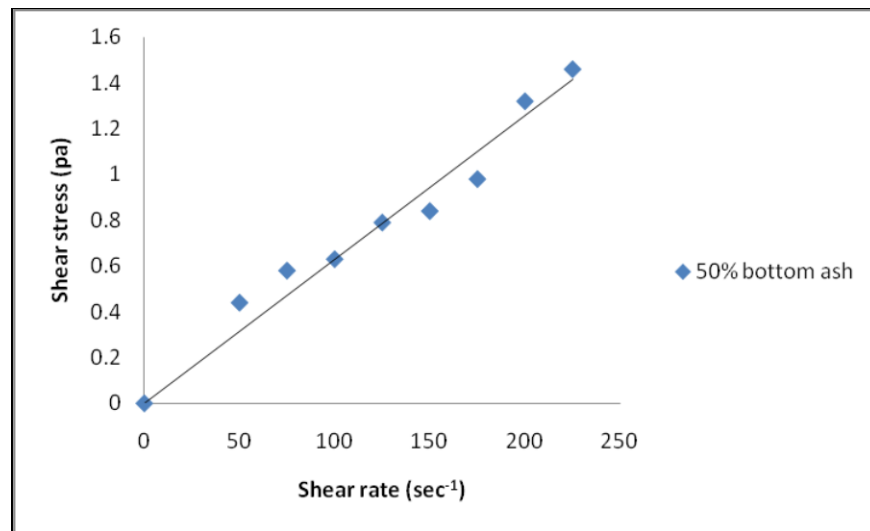


Figure 4.4: Rheology of bottom ash slurry sample with variation of concentration such as (a) 10% bottom ash (b) 20% bottom ash (c) 30% bottom ash (d) 40% bottom ash (e) 50% bottom ash

4.3 SEM Analysis

SEM analysis of bottom ash is done in respect to check its shape and size, as erosion depends upon size and shape of erodent particle. As clear from Figure 4.5 the ash particles are approximately circular in nature. Some sharp edges are seen which are responsible for erosion.

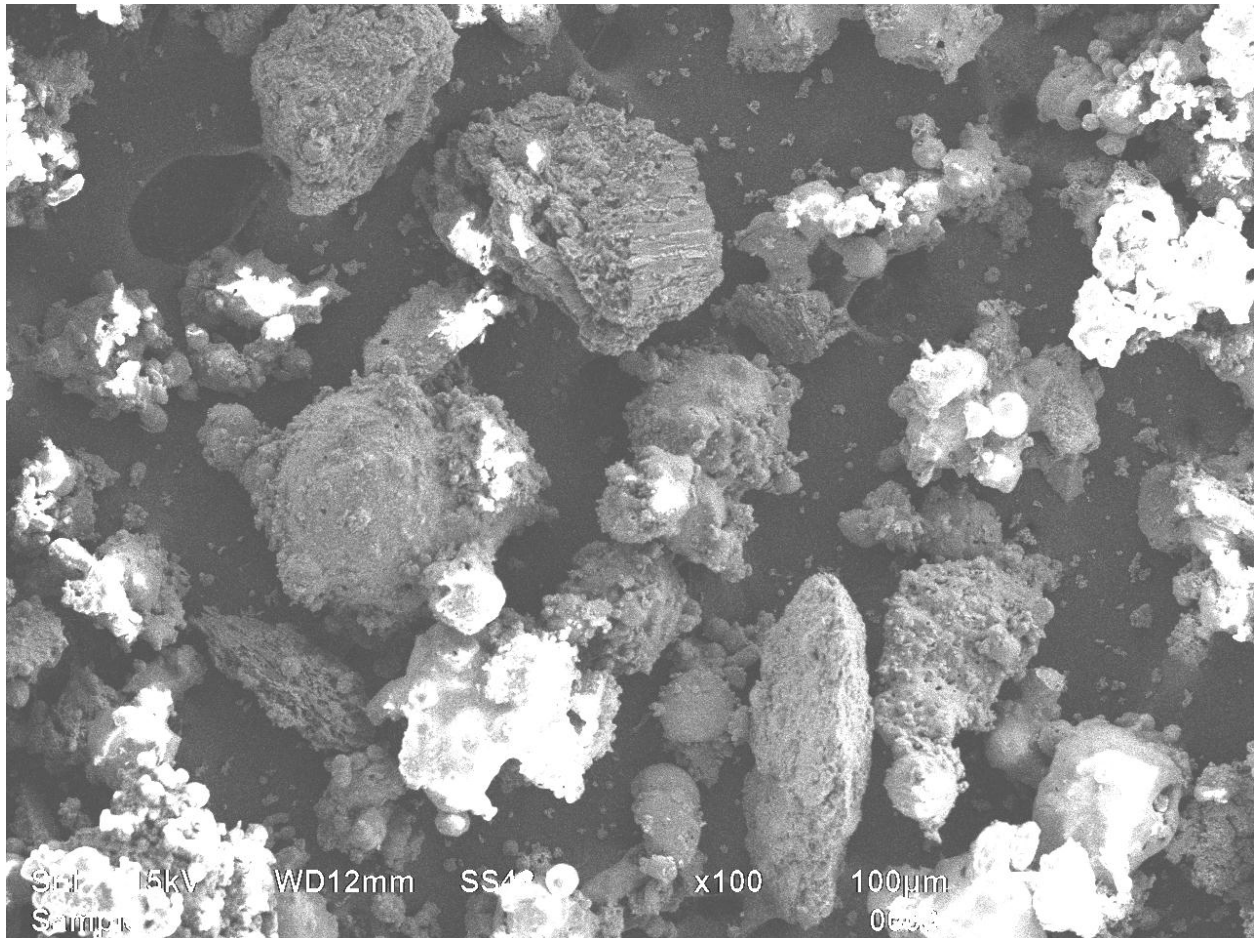


Figure 4.5: SEM analysis of bottom ash

5.1 EROSION OF MILD STEEL

5.1.1 Weight Loss with respect to Time

Erosion wear of mild steel can be calculated by varying various parameters such as impact angle, mass flow rate or the time. The amount of eroded material is calculated by calculating the weight lost after the testing of a sample of a given material. And the observations are shown with the help of graphs representing weight loss of a material with respect to the time. The weight loss at different flow rates with variation of impact angles are shown in Figure 5.1- 5.3. It is observed that erosion wear rate (weight loss) increases with respect to time.

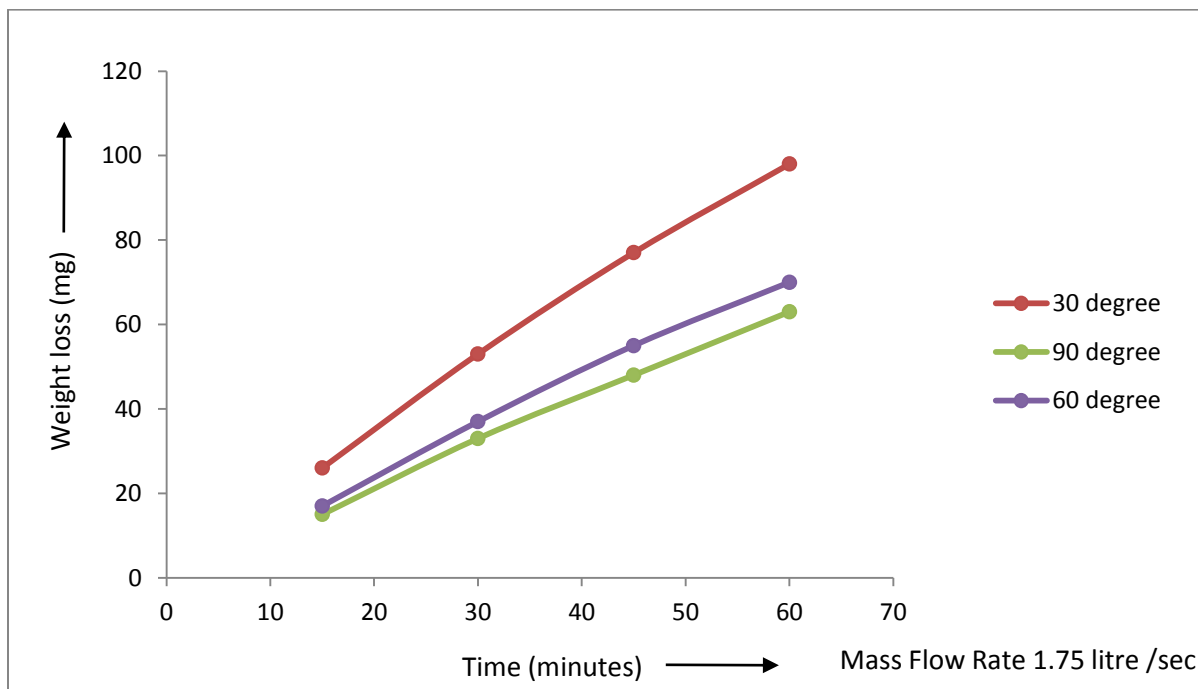


Figure 5.1:Weight Loss w.r.t Time

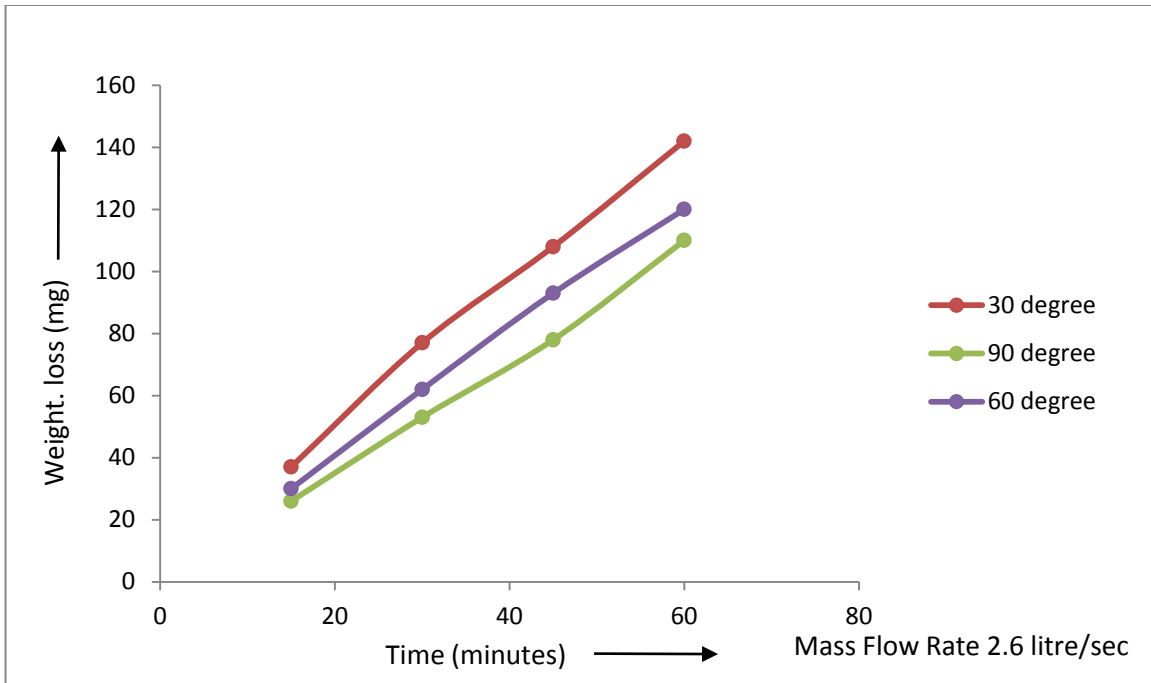


Figure 5.2: Weight Loss w.r.t Time

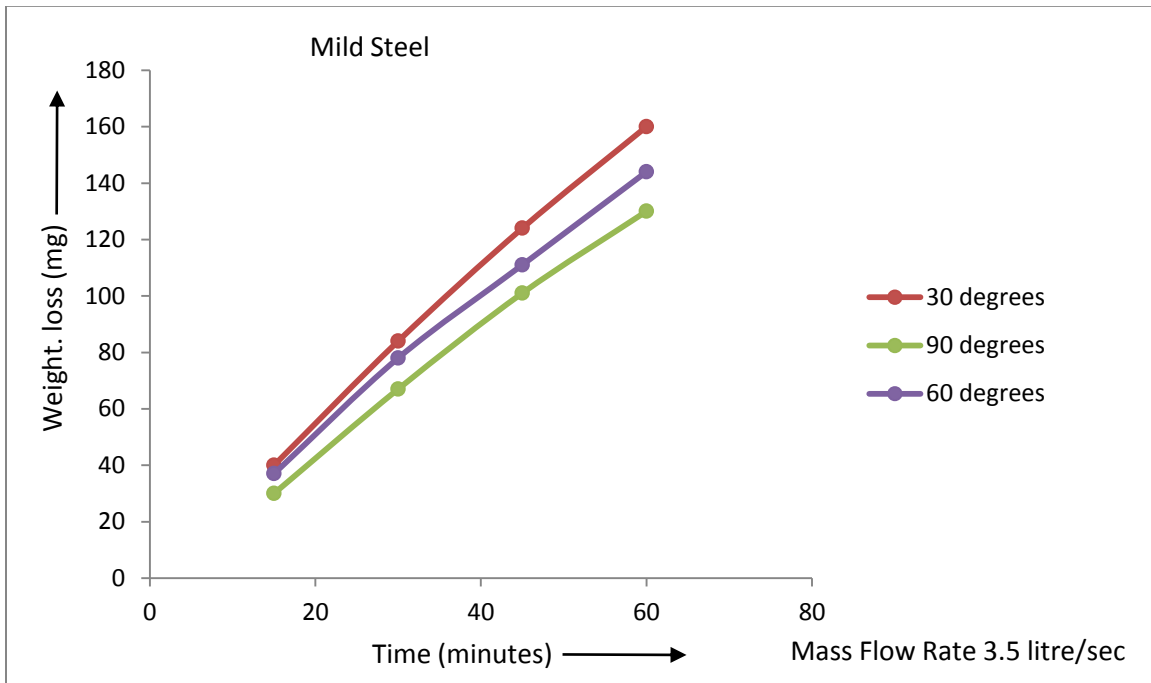


Figure 5.3: Weight Loss w.r.t Time

5.1.2 Effect of Velocity

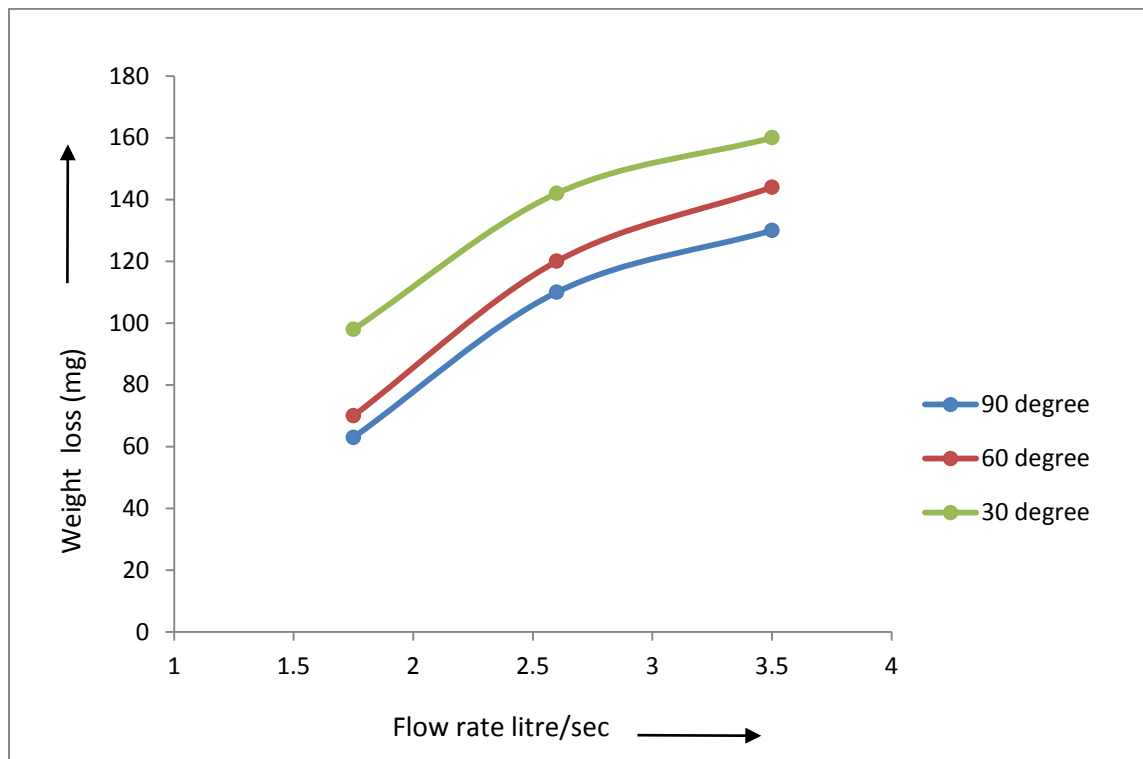


Figure 5.4: Effect of velocity on mild steel

Figure 5.4 shows that weight loss increases with the velocity of bottom ash slurry. The weight loss is twice when flow rate is increased from 1.75 litre /sec to 2.6 litre /sec than increased from 2.6 litre/sec to 3.75 litre /sec. As velocity increase, the kinetic energy of solid particle of erodent also increases which results in more weight loss.

5.1.3 Effect of Angle.

Impact angle plays the significant role in deciding the weight loss and mechanism of erosion. Effect of angle is shown in Figure 5.5. At lower angles mechanism of erosion is micro cutting and ploughing and at higher angle mechanism of erosion is fatigue and fracture.

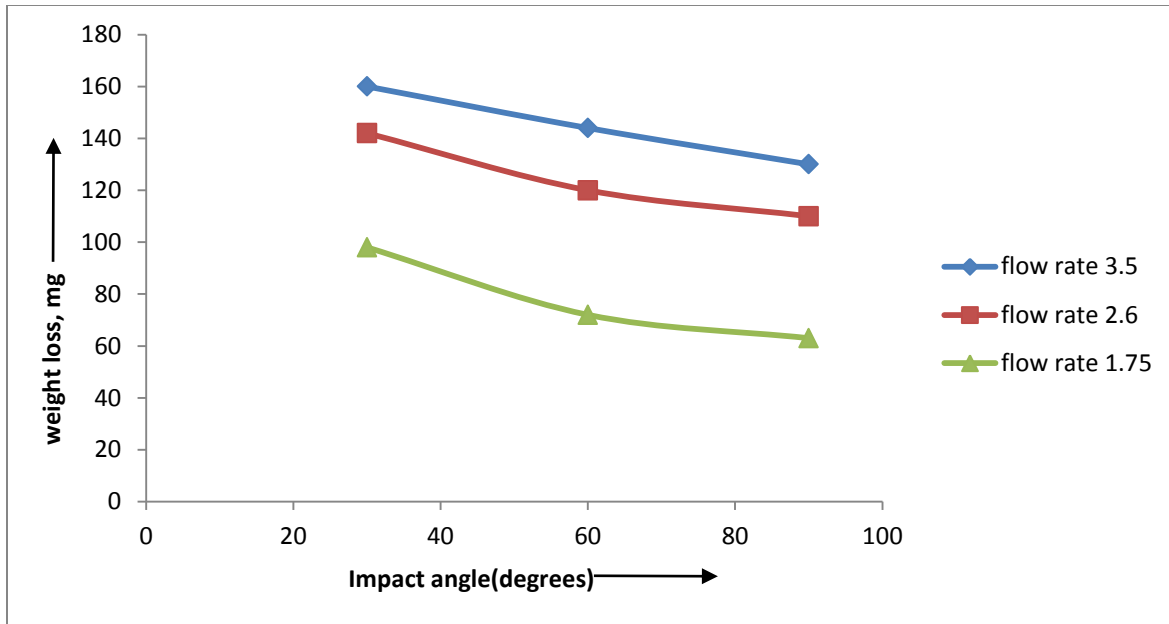


Figure 5.5: Effect of Angle on Mild Steel

From Figure 5.5 it is observed that the maximum weight loss is at angle of 30° and minimum at 90° . Same trend is followed at all levels of mass flow rate. At lower angle tangential component of velocity causes the erosion and at higher angle normal component is responsible for the erosion.

5.1.4 SEM analysis of Mild Steel

A scanning electron microscope (SEM) is a type of electron microscope that images a sample by scanning it with a high-energy beam of electrons. The electrons interact with the atoms that make up the sample producing signals that contain information about the sample's surface topography, composition, and other properties such as electrical conductivity. The samples of material used for erosion purpose was examined with help of scanning electron microscope with aim to visualize change in microstructure in order to know the mechanism of erosion. The SEM of mild steel before erosion and after erosion are given below:

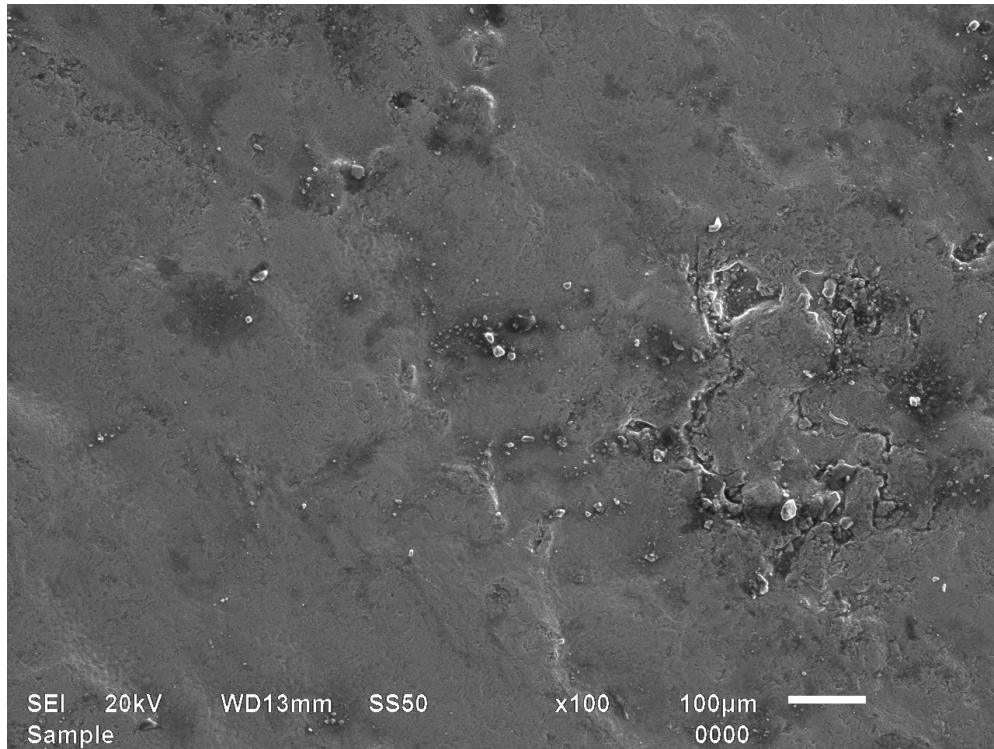


Figure 5.6: SEM of mild steel before wear

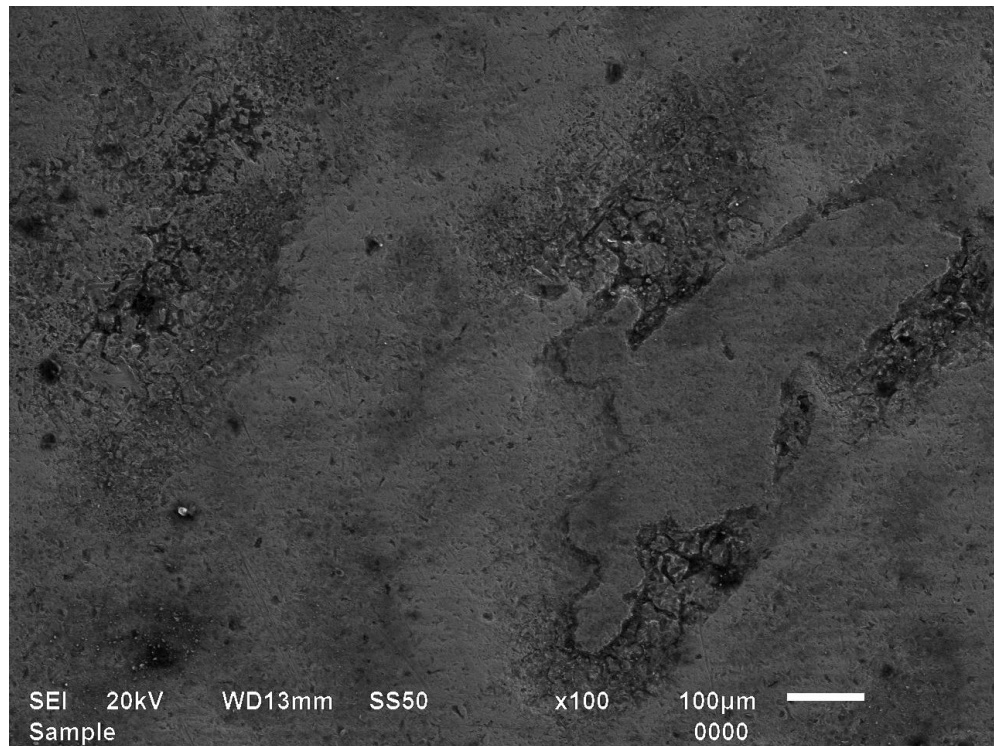


Figure 5.7: SEM of mild steel after wear

5.2 EROSION OF GREY CAST IRON

5.2.1 Weight Loss with respect to Time

Erosion wear of grey cast iron can be calculated by varying various parameters such as impact angle, mass flow rate or the time. The amount of eroded material is calculated by calculating the weight lost after the testing of a sample of a given material. The weight loss of materials depends on property of material like ductility, hardness, strength, etc. And the observations are shown with the help of graphs representing weight loss of a material with respect to the time. The following graphs (Figure 5.8, 5.9, 5.10) represent the weight loss at different flow rates with similar parameters.

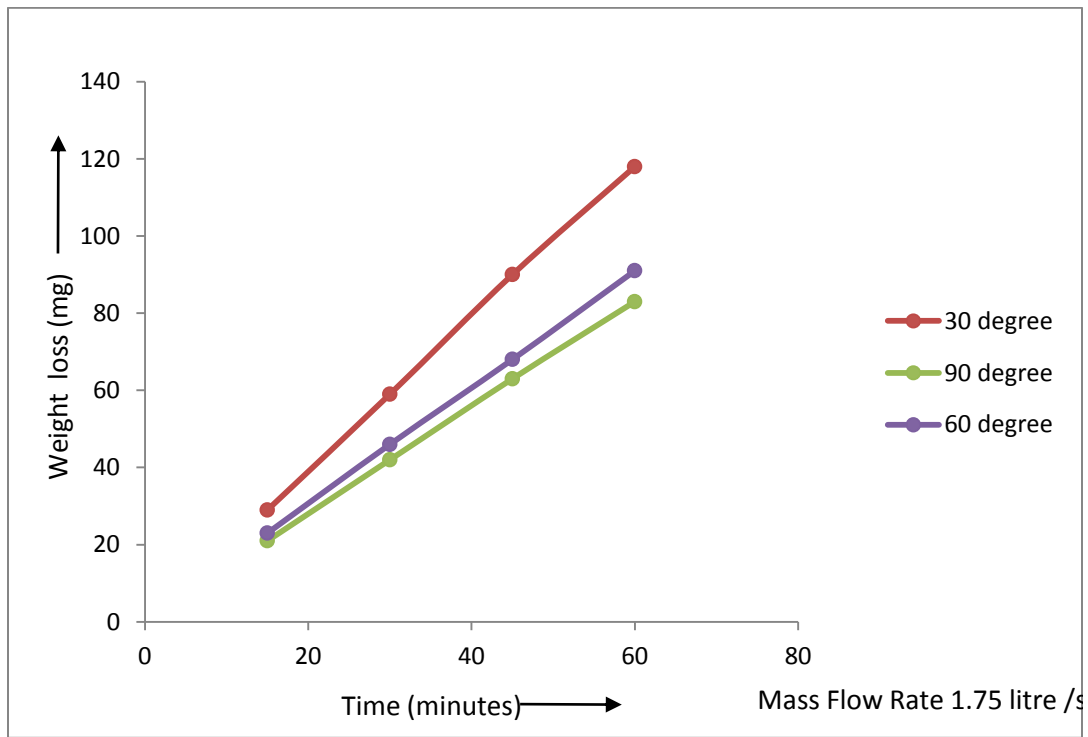


Figure 5.8: Weight Loss w.r.t Time

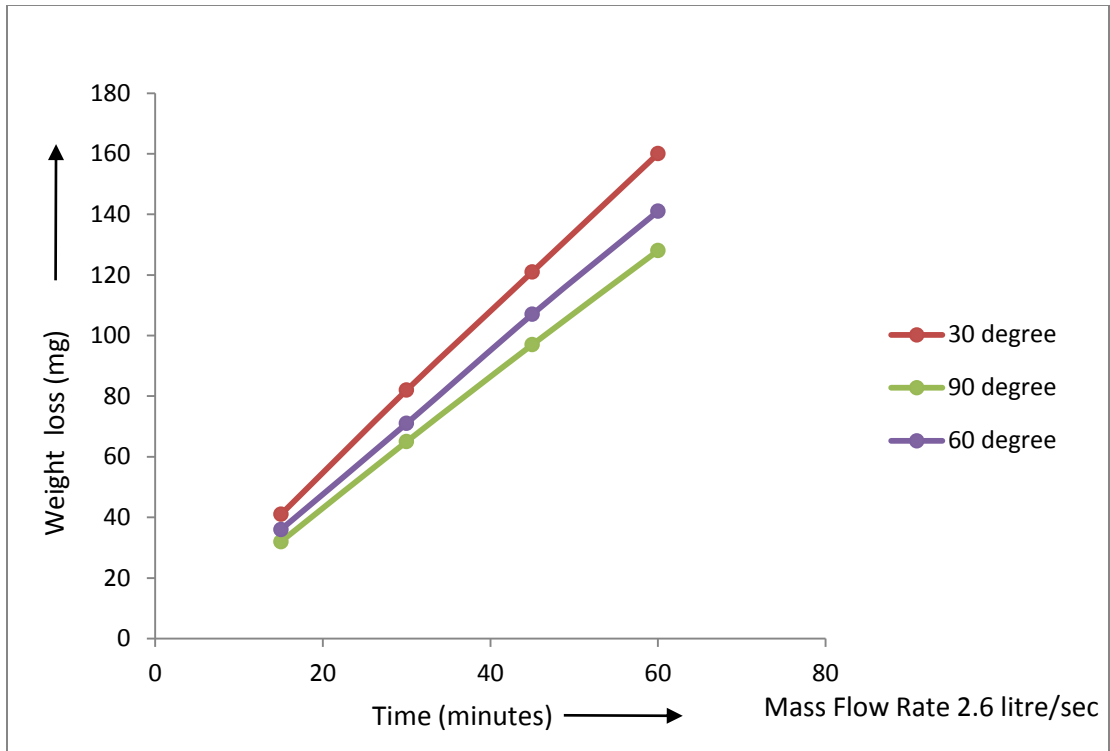


Figure 5.9: Weight Loss w.r.t Time

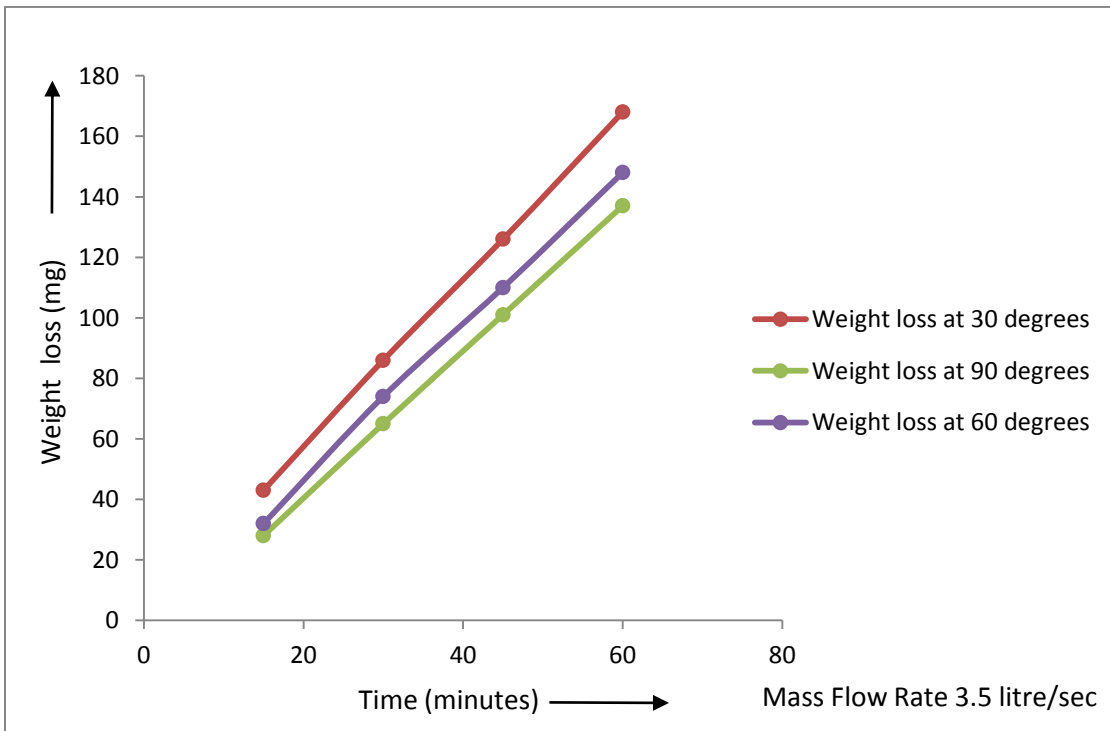


Figure 5.10: Weight Loss w.r.t Time

Weight loss increases with increase in time. The rate of weight loss is almost uniform in Figure 5.8. The slope of curve representing the weight loss w.r.t time at 30° impact angle is much steeper than the other two but the weight loss rate is constant. In Figure 5.9 points of weight loss after fifteen minutes of testing are overlapping each other which means weight loss has been almost same in the initial time period. Figure 5.10 shows almost the constant weight lost throughout the time span.

5.2.2 Effect of Velocity

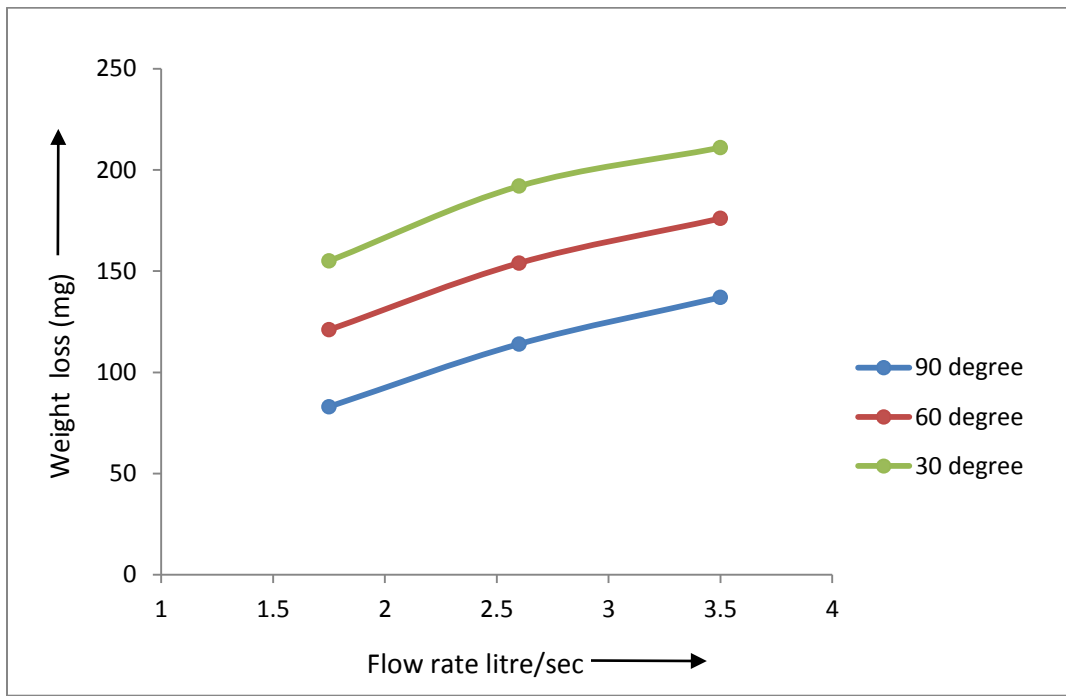


Figure 5.11: Effect of velocity

It is clear from the Figure 5.11 that weight loss increases as the velocity is increased. When the flow rate is increased from lower level to medium level the weight loss is twice as compared to the weight loss when flow rate is increased to higher level. Higher the velocity more is the kinetic energy for deformation and removal of material.

5.2.3 Effect of angle.

Impact angle plays the significant role in deciding the weight loss and mechanism of erosion. Effect of angle is shown in Figure 5.12. At lower angles mechanism of erosion is micro cutting and ploughing and at higher angle mechanism of erosion is fatigue and fracture.

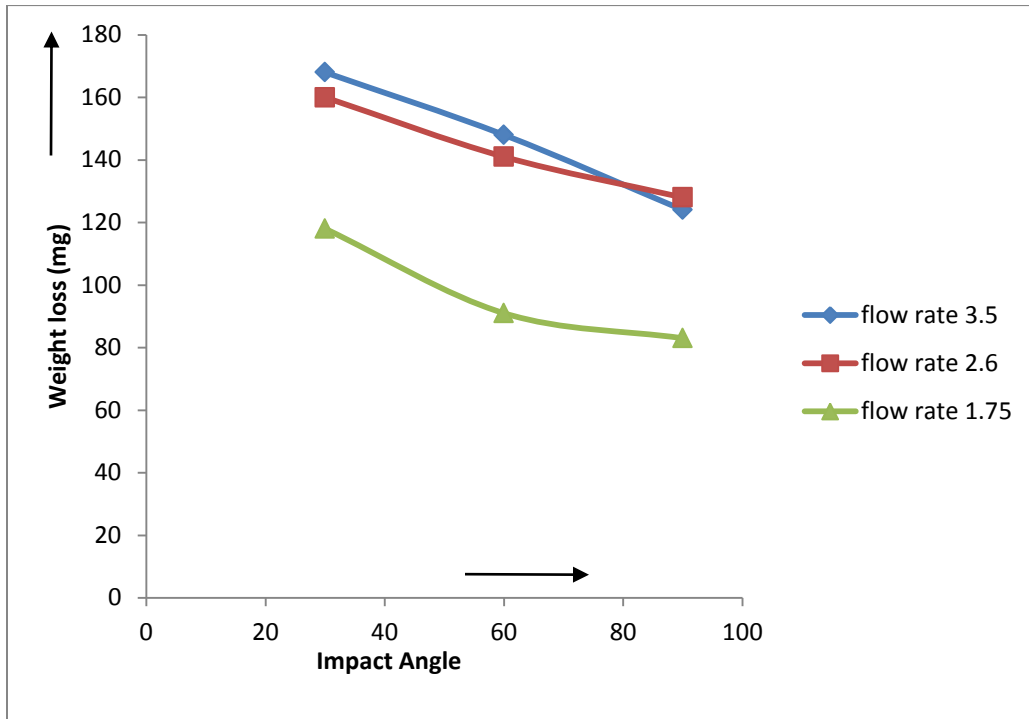


Figure 5.12: Effect of Impact Angle

The maximum weight loss of material is at 30° and minimum at 90° because of its ductile nature. The weight loss at 90° for the flow rate 2.6 litre/second is more than the weight loss at flow rate 3.5 litre/second. As the flow is increased from 2.6 litre/second to 1.75 litre/second significant increase in weight loss is observed but in 2.6 litre/second and 3.5 litre/second only marginal difference is found at all the angles.

5.2.4 SEM analysis of Grey Cast Iron

The following figures show the microstructure of 13Cr-4Ni Stainless Steel before and after wear. Figure 5.13 and 5.14 clearly shows that the erosion of material is by micro cutting and ploughing mechanism.

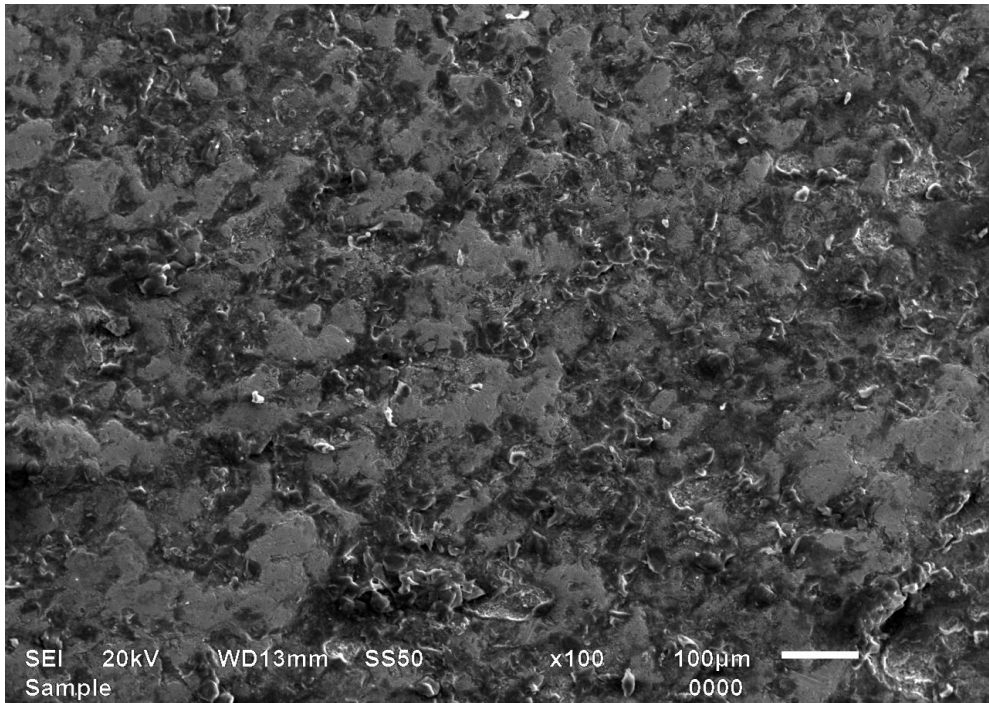


Figure 5.13: SEM of grey cast iron before wear

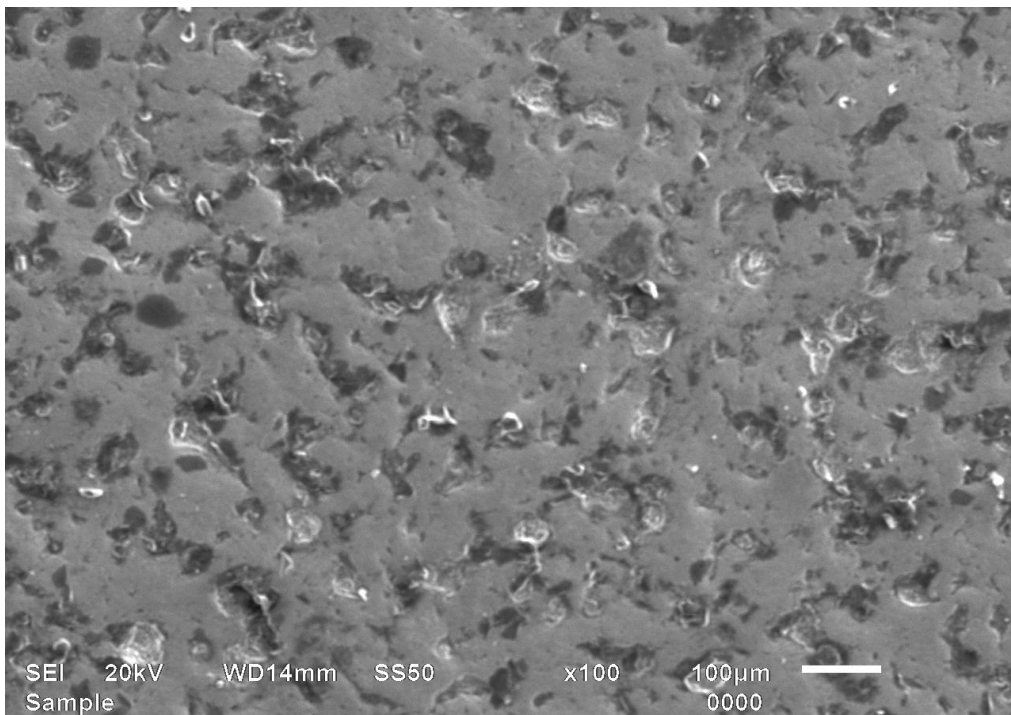


Figure 5.14: SEM of grey cast iron after wear

5.3 EROSION OF 13Cr-4Ni STAINLESS STEEL

5.3.1 Weight Loss with respect to Time

Erosion wear of mild steel can be calculated by varying various parameters such as impact angle, mass flow rate or the time. The amount of eroded material is calculated by calculating the weight lost after the testing of a sample of a given material. And the observations are shown with the help of graphs representing weight loss of a material with respect to the time. The following graphs (Figure 5.15, 5.16, 5.17) represent the weight loss at different flow rates with similar parameters.

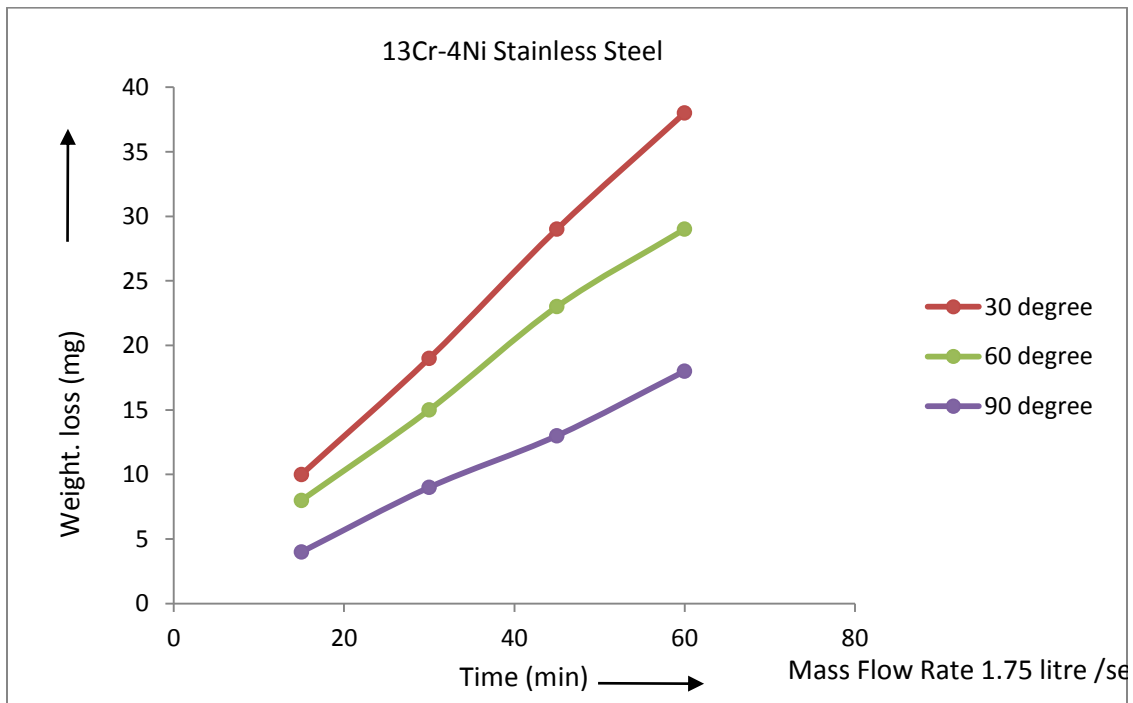


Figure 5.15: Weight loss w.r.t Time

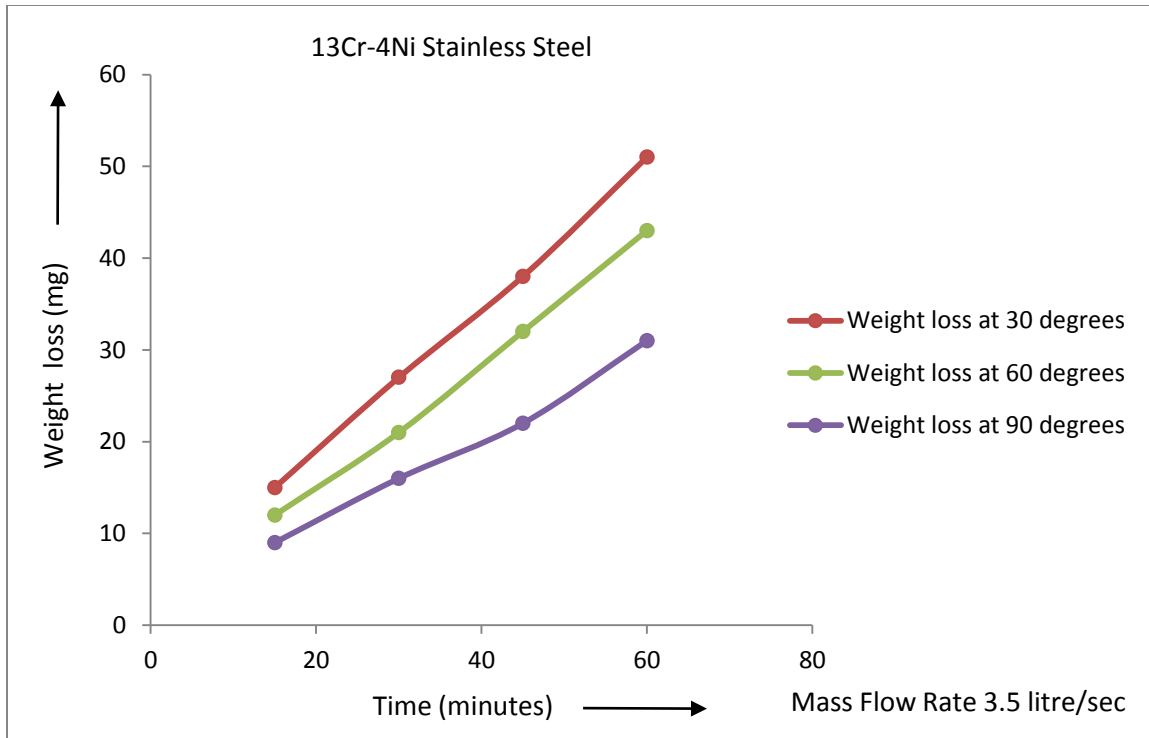


Figure 5.16: Weight loss w.r.t Time

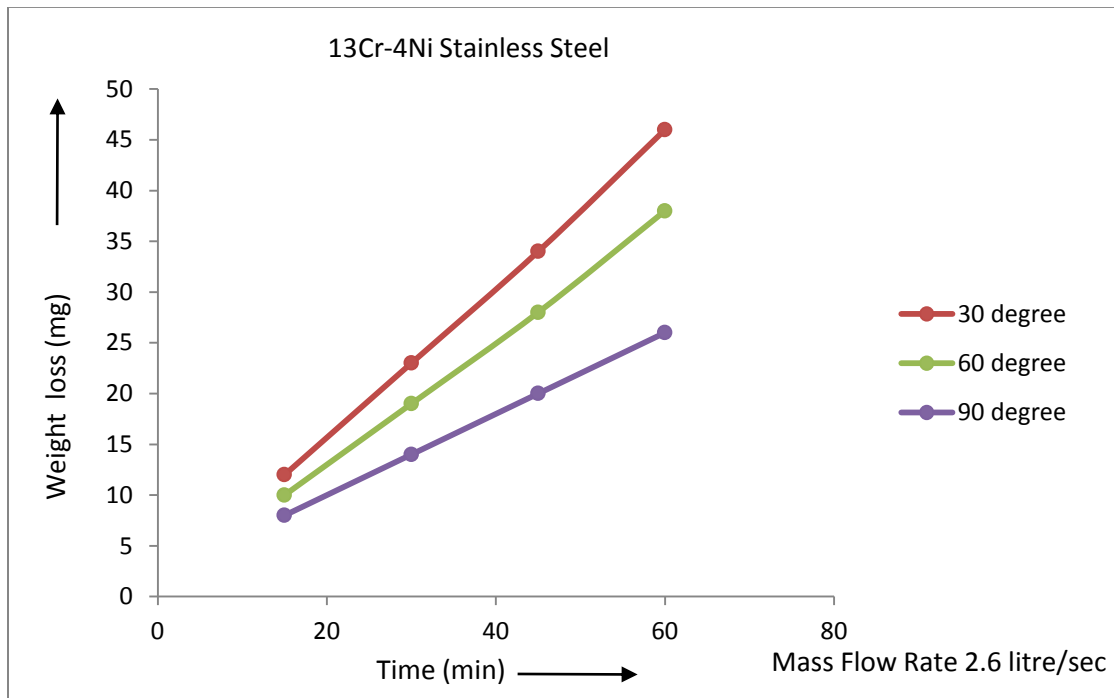


Figure 5.17: Weight loss w.r.t Time

Figures 5.14-5.17 represent the weight loss w.r.t time at different angle and flow rates. The weight loss curve at 90° shows high weight loss rate initially but after 30 minutes the weight loss rate decreases. All other curves shows the linear trend i.e. nearly constant weight loss rate. In starting period of 15 minutes the difference in weight loss is small but as the time progress the difference in weight loss increases. It shows that due to repetitive action of slurry the surface of material may loss its strength thus more weight loss as the time progress. The flow rate affects the weight loss but the overall trend is almost same in all the graphs shown above.

5.3.2 Effect of velocity

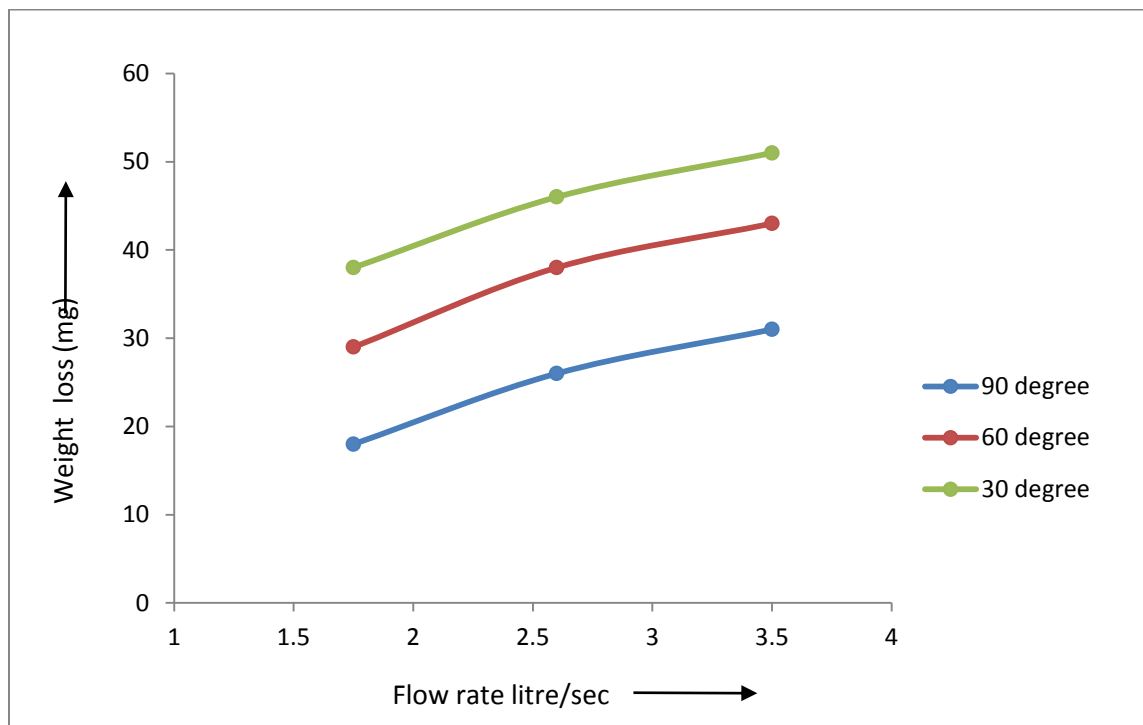


Figure 5.18: Effect of Velocity

The fig clearly states that the weight loss increases with increase in flow rate. The same trend is followed by the curve at each flow rate. 60% of total weight loss is observed when flow is increased from 1.75 litres/second to 2.6 litres/second.

5.3.3 Effect of impact angle

The impact angle is important parameter. If material is ductile max erosion is at 30° and for brittle materials maximum erosion is assumed to be at 90°. The result of weight loss with respect to angle is shown in Figure 5.19.

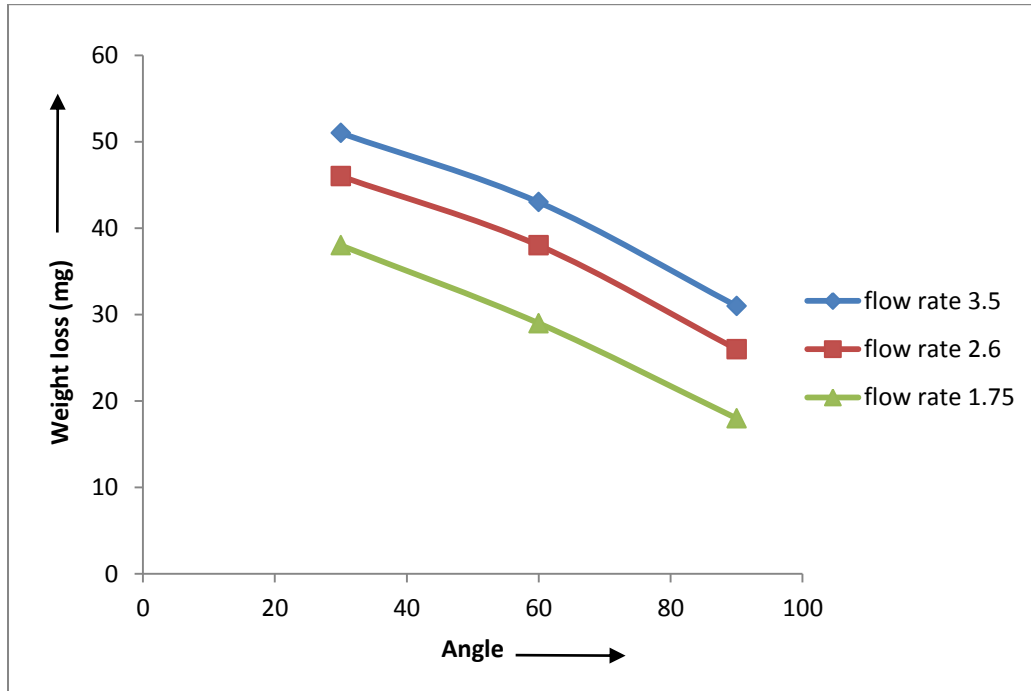


Figure 5.19: Effect of Impact Angle

The graph shows that maximum erosion is at 30° and erosion decreases by increase in angle. The minimum erosion is at 90°. And this trend is followed at all different levels of flow rate. This shows that 13Cr-4Ni steel is ductile in nature.

5.3.4 SEM analysis of 13Cr- 4Ni Stainless Steel

The following figures show the microstructure of 13Cr-4Ni Stainless Steel before and after wear. Figure 5.20 and 5.21 clearly shows that the erosion of material is by micro cutting and ploughing mechanism.

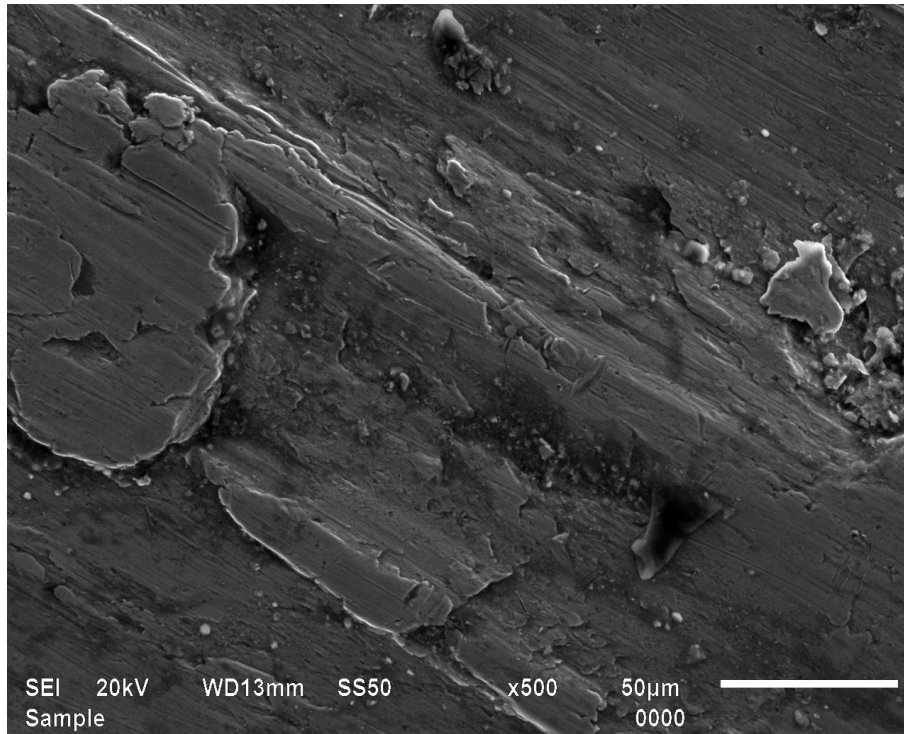


Figure 5.20: SEM of 13 Cr-4Ni Stainless Steel before wear

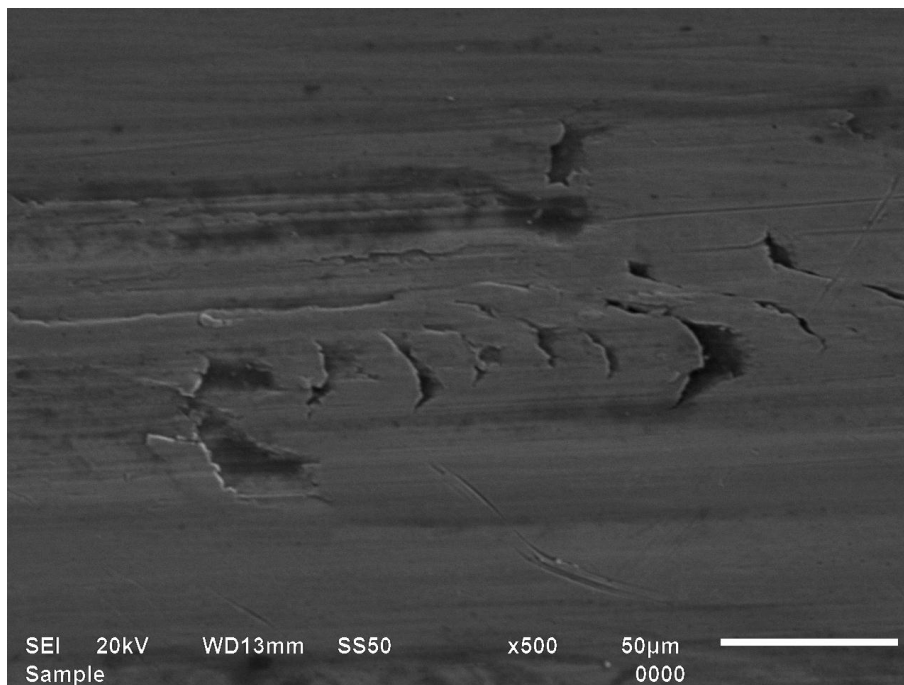


Figure 5.21: SEM of 13 Cr-4Ni Stainless Steel after wear

5.4 EROSION OF 16Cr-5Ni STAINLESS STEEL

5.4.1 Weight Loss with respect to Time

16Cr-5Ni stainless steel is known for its good resistance against erosion wear. Erosion wear of 16Cr-5Ni stainless steel is calculated by varying various parameters. Figures 5.22-5.24 represent the weight loss with respect to time at different angle and flow rates. The weight loss curve at 90° shows high weight loss rate in starting but after 30 minutes the weight loss rate decreases. All other curves shows the linear trend i.e. nearly constant weight loss rate. In starting period of 15 minutes the difference in weight loss is small but as the time progress the difference in weight loss increases. It shows that due to repetitive action of slurry the surface of material may lose its strength thus more weight loss as the time progress. The flow rate affects the weight loss but the overall trend is almost same in all the graphs shown below.

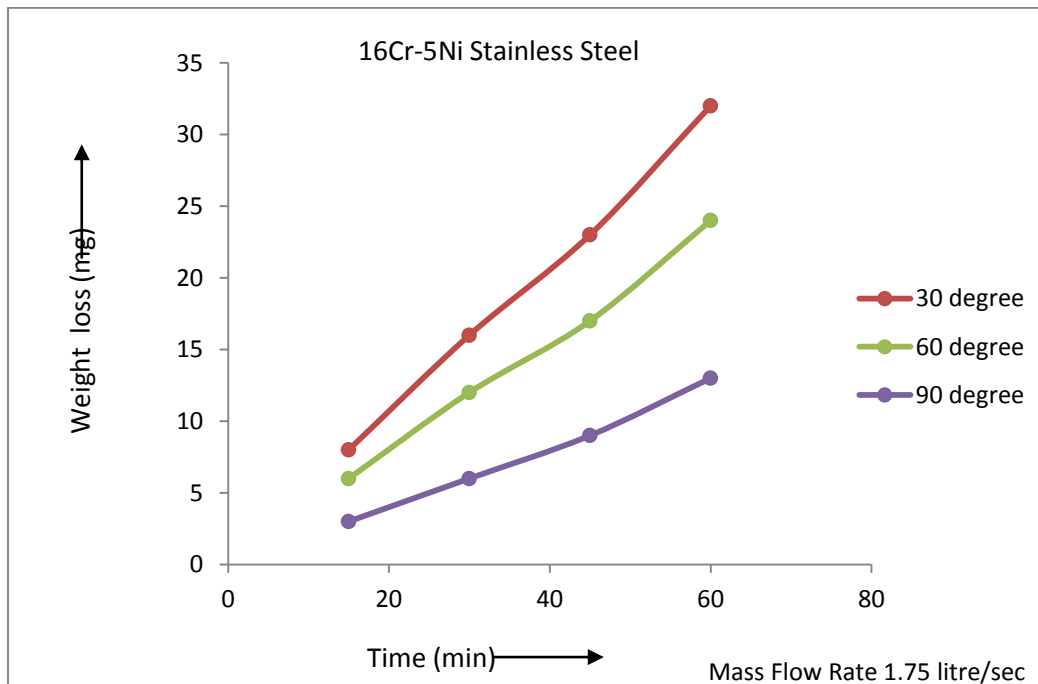


Figure 5.22: Weight loss w.r.t Time

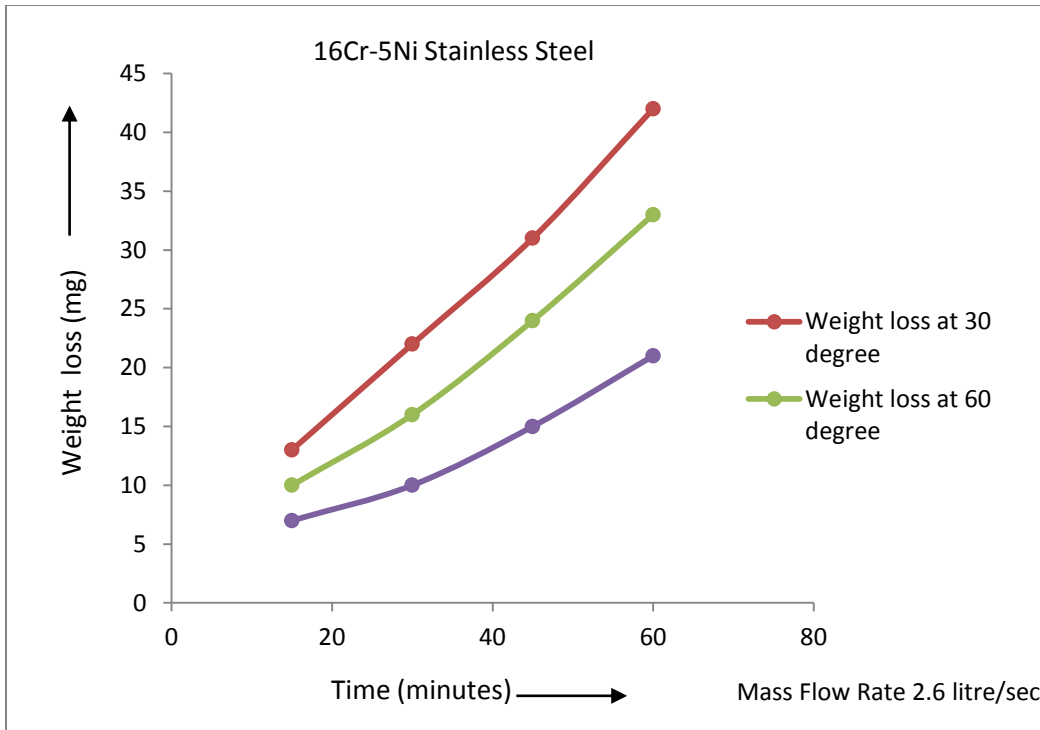


Figure 5.23: Weight loss w.r.t Time

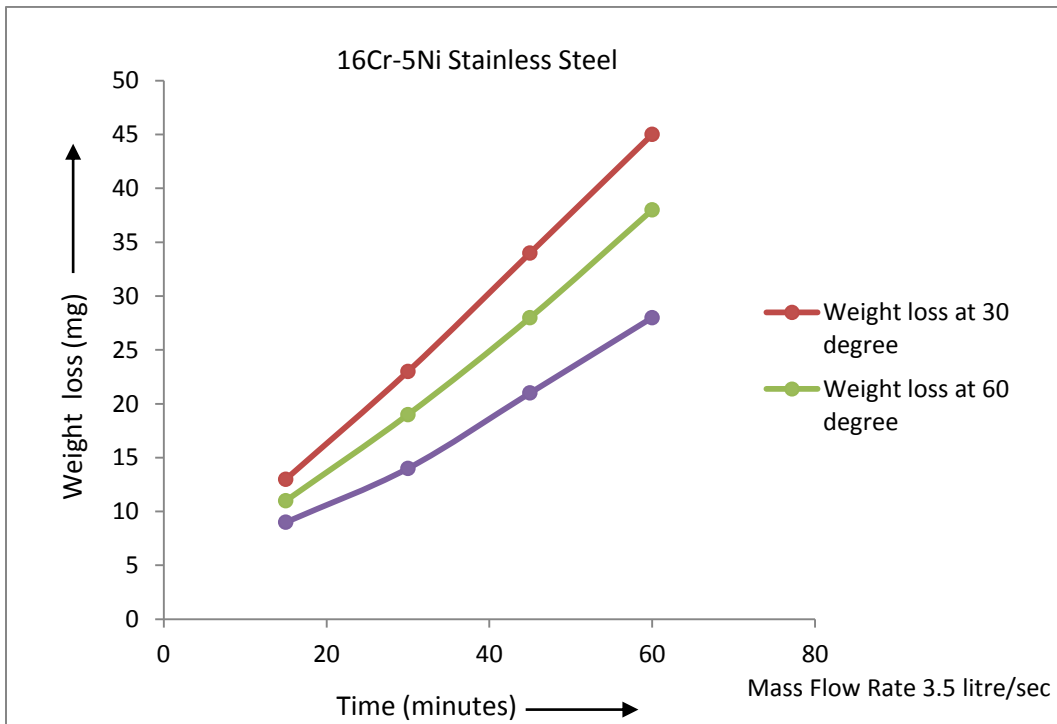


Figure 5.24: Weight loss w.r.t Time

5.4.2 Effect of velocity

With the increase in velocity of flow the weight loss the material increase as shown in Figure 5.25. At an angle of 30°, the weight loss in second increment of velocity is almost half then the first increment. At 90° nearly equal amount of weight is lost in both changes. The increase in erosion may differ with every increase in velocity but increase in wear is sure.

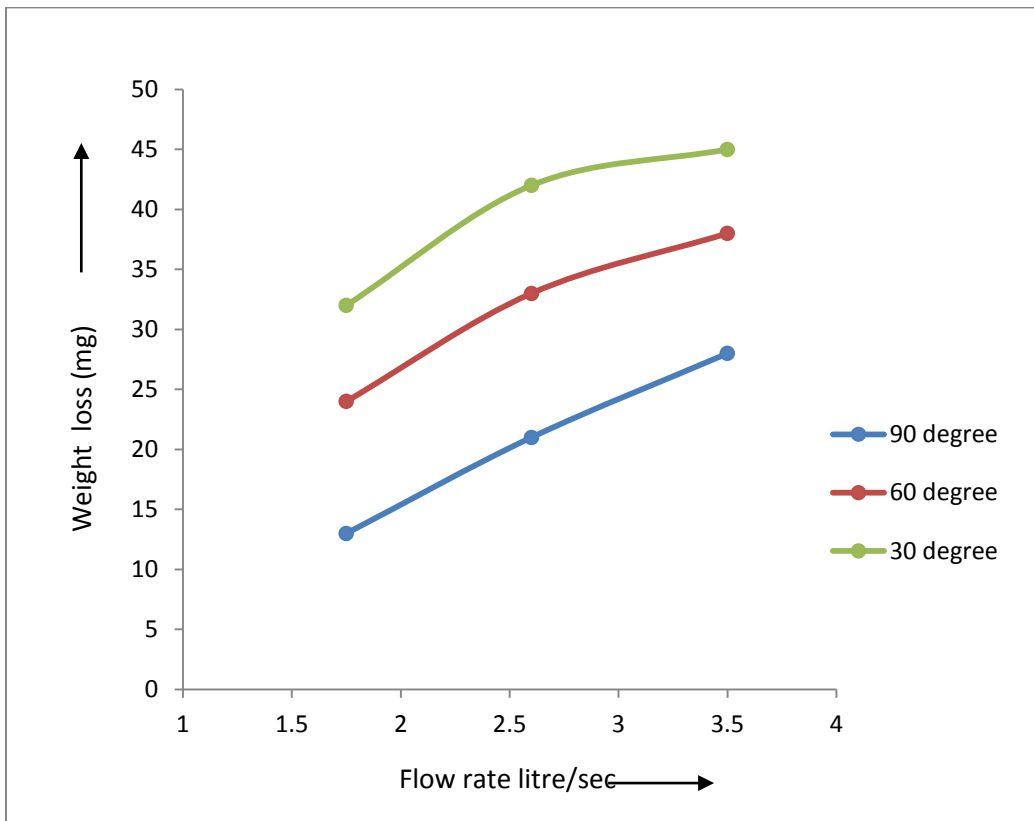


Figure 5.25: Weight loss w.r.t Velocity

5.4.3 Effect of Impact Angle

The effect of impact angle for the 16Cr-5Ni Stainless Steel is shown in Figure 5.20. This shows that weight loss decreases with increase in angle. The weight loss is maximum at 30° and minimum at 90°.

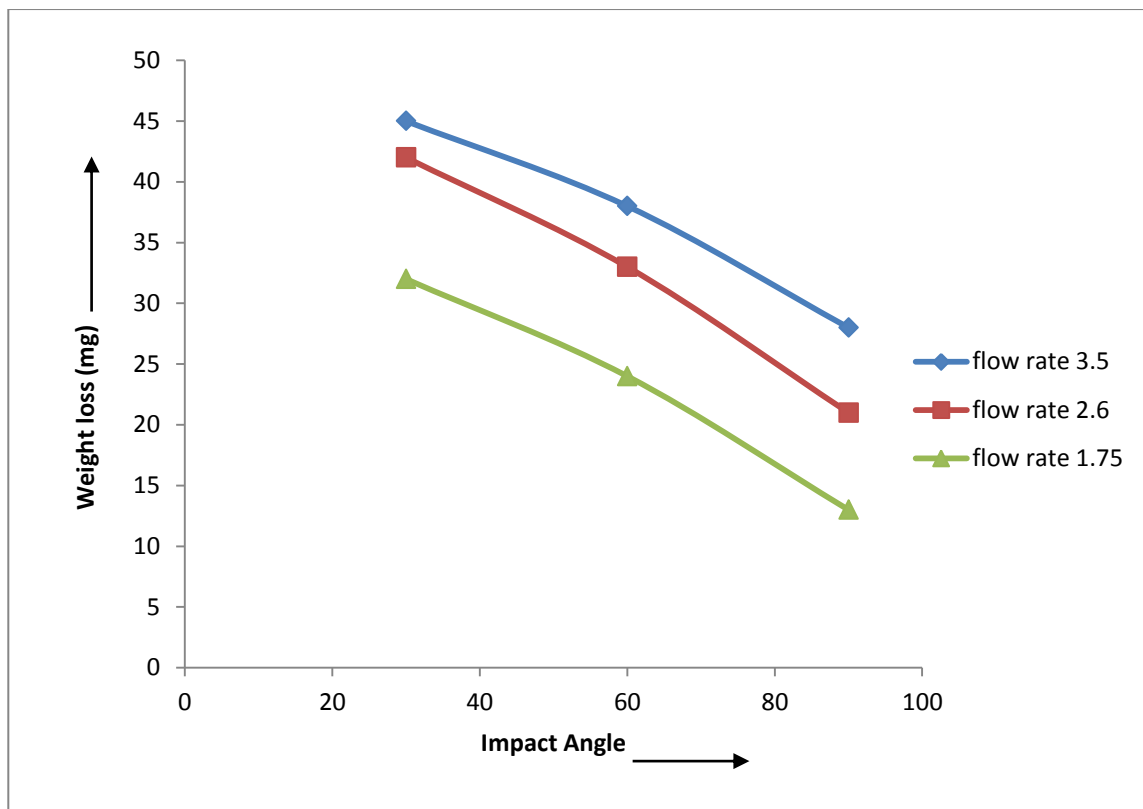


Figure 5.26: Effect of Impact Angle

5.4.4 SEM analysis of 16Cr-5Ni Stainless Steel

The following figures show the microstructure of 16Cr-5Ni Stainless Steel before and after wear. Figure 5.27 and 5.28 clearly shows that the erosion of material is by ploughing mechanism. As the materials are ductile in nature so erosion has to be by micro cutting and ploughing mechanism.

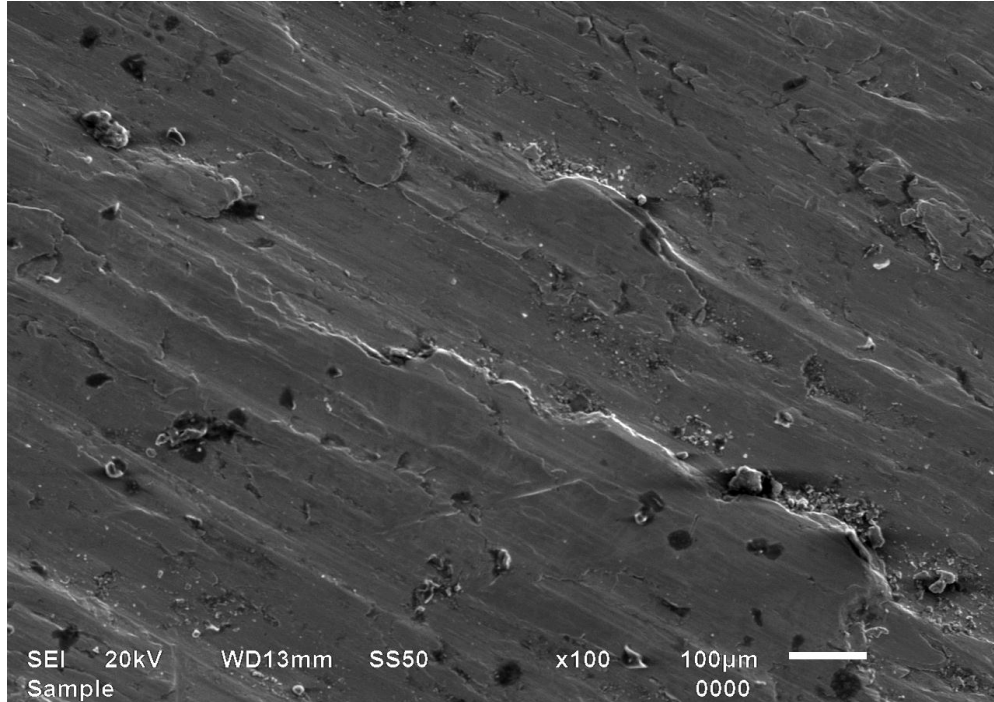


Figure 5.27: SEM of 16Cr-5Ni Stainless Steel before wear

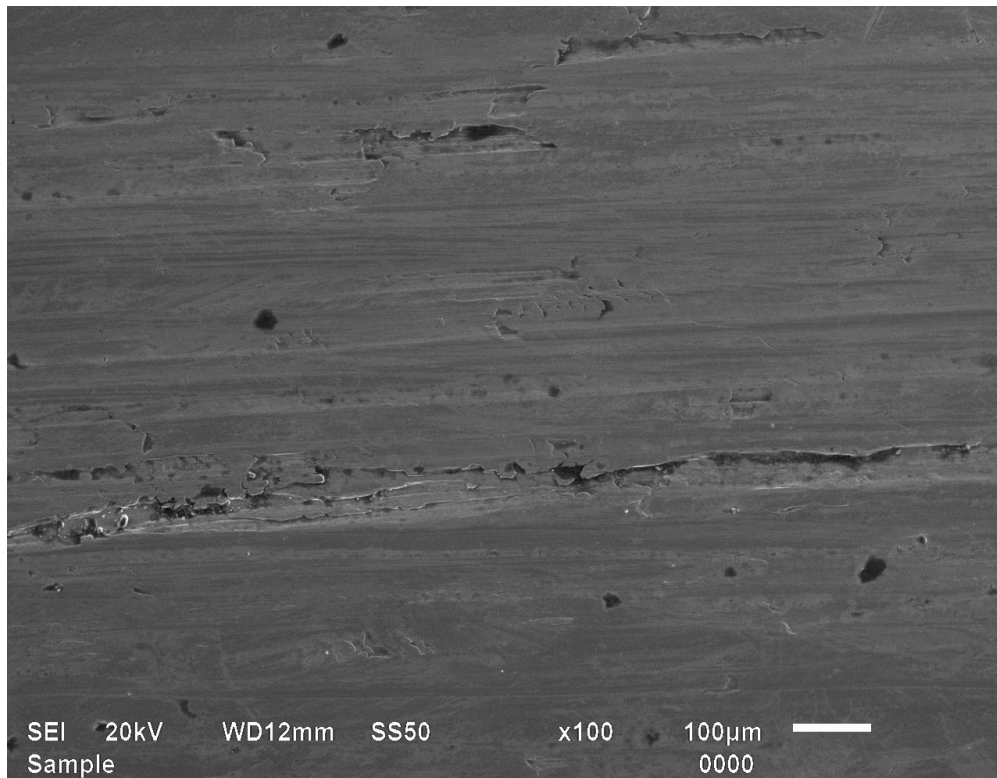


Figure 5.28: SEM of 16Cr-5Ni Stainless Steel after wear

5.5 COMPARISON OF THE MILD STEEL, GREY CAST IRON, 13Cr-4Ni STAINLESS STEEL & 16Cr-5Ni STAINLESS STEEL

5.5.1 Erosion with respect to Time

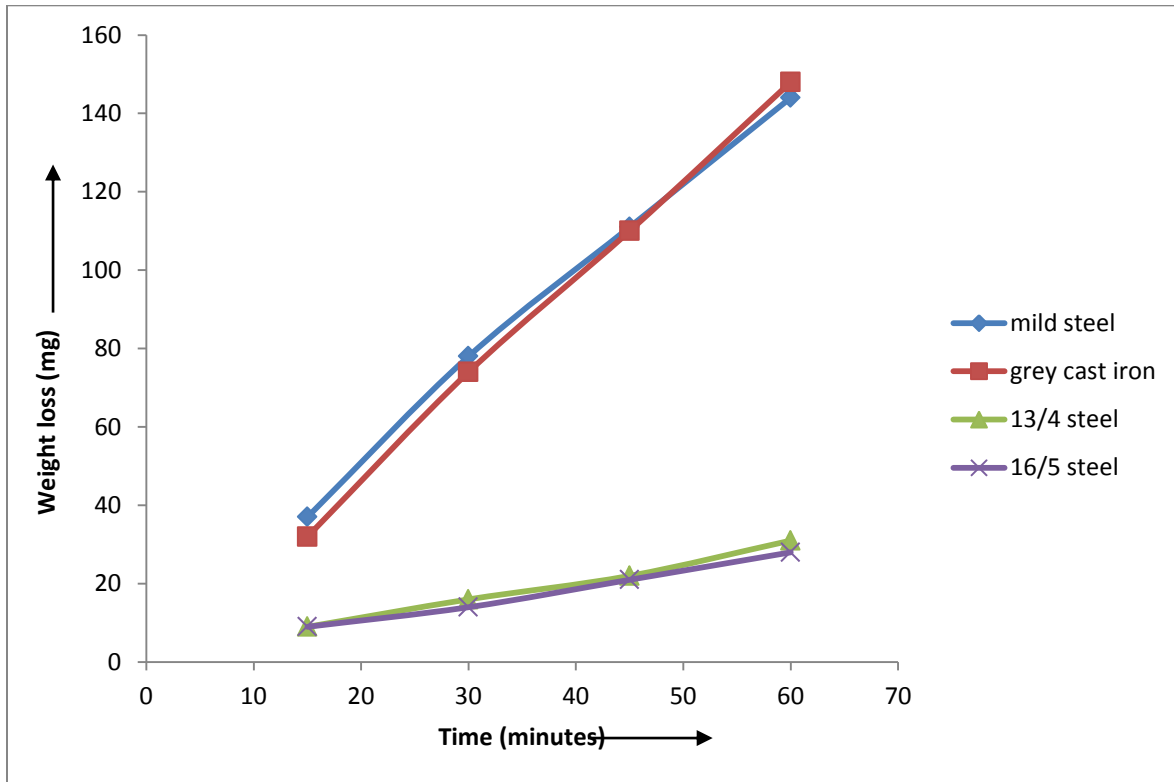


Figure 5.29: Erosion with respect to Time

The above graph shows the erosion experienced by all the four materials namely Mild Steel, Grey Cast iron, 13Cr-4Ni Stainless Steel and 16Cr-5Ni Stainless Steel with time when tested on a Erosion Jet Tester. The materials 13Cr-4Ni Stainless Steel and 16Cr-5Ni Stainless Steel, being hard and ductile in nature experience very less erosion with the passage of time whereas the other two materials, Mild Steel and Grey Cast iron, being less harder erode more with respect to time. There is a significant difference in erosion being observed between these two groups of materials.

5.5.2 Erosion with respect to Mass Flow Rate

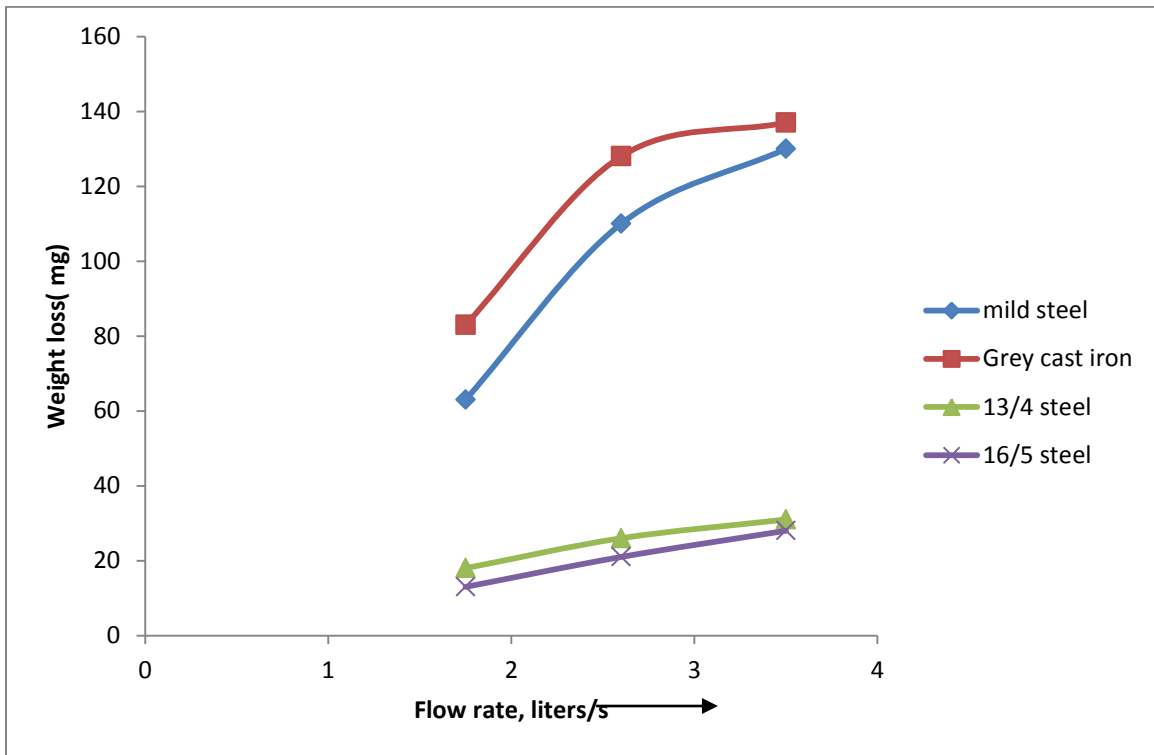


Figure 5.30: Erosion with respect to Mass Flow Rate

The above graph shows the erosion experienced by all the four materials namely Mild Steel, Grey Cast iron, 13Cr-4Ni Stainless Steel and 16Cr-5Ni Stainless Steel with constantly increasing mass flow rate or the velocity of the erodent coming out of the jet of a Erosion Jet Tester. The materials 13Cr-4Ni Stainless Steel and 16Cr-5Ni Stainless Steel, show constant erosion rate throughout. At the maximum velocity their erosion is almost same. However the other two materials, Mild Steel and Grey Cast Iron, erode more with increasing velocity. These two materials also show a high rate of erosion initially and then the erosion rate stabilises and increases gradually. respect to time. There is a significant difference in erosion being observed between these two groups of materials.

5.5.3 Erosion with respect to varying Impact Angle

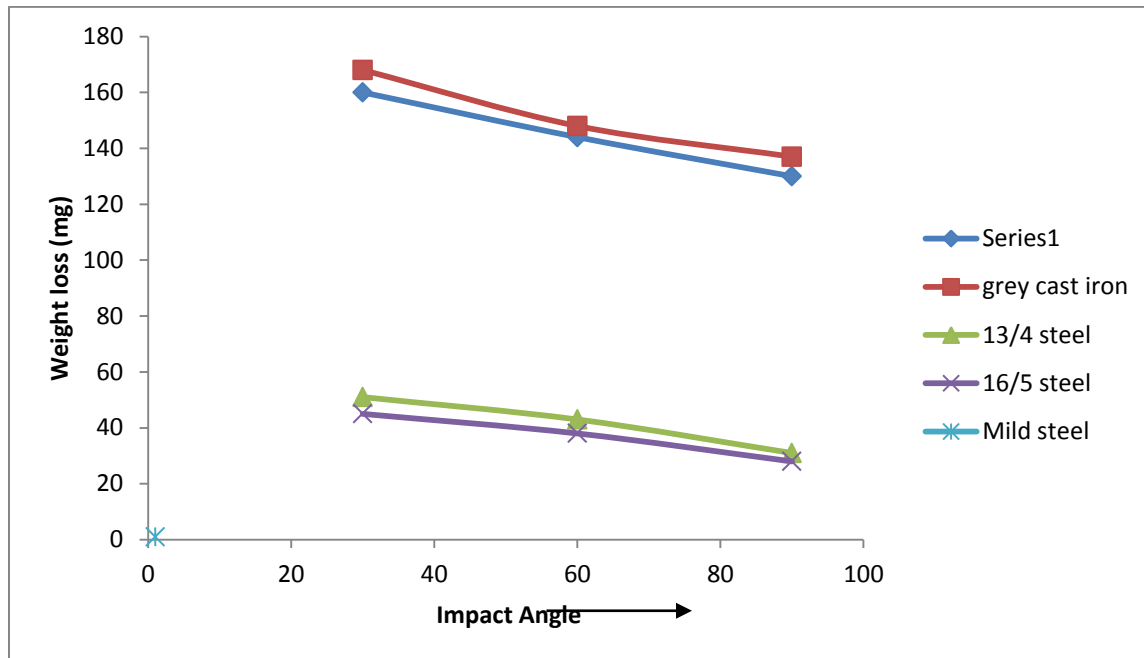


Figure 5.31: Erosion with respect to varying Impact Angle

The above graph shows that for all the four materials the weight loss decreases with increase in angle. Mild Steel and Grey Cast Iron have higher erosion rate as compared to 16 Cr- 5 Ni and 13 Cr-4 Ni stainless steel.

CONCLUSIONS AND FUTURE SCOPE

The parametric study of erosion wear for the materials Mild Steel, Grey Cast iron, 13Cr-4Ni Stainless Steel and 16Cr-5Ni Stainless Steel is studied by experimentation using Jet tester and it is concluded that :

- Erosion wear is a function of velocity of slurry. As velocity increases erosion wear rate proportionally increases.
- 16Cr-5Ni Stainless Steel has the least erosion wear compared to other selected materials Mild Steel, Grey Cast iron, 13Cr-4Ni Stainless Steel and grey cast iron erosion wear is found maximum.
- Maximum erosion wear rate is found at impact angle 30° and minimum at impact angle 90°.
- Erosion wear weight loss is the function of time.
- The materials 13Cr-4Ni Stainless Steel and 16Cr-5Ni Stainless Steel shows similar behaviour towards erosion and Mild Steel and Grey Cast iron also shows identical behaviour

Future Work.

- The same erosion wear studies can be performed with coatings of different materials and also can be studied with different type of coating processes.
- The computational approach can be used to simulate the similar work with different operating conditions.
- The effect of erosion wear of pump impeller and hydro turbine blade can be studied.
- The same erosion wear studies can be extended with variation of concentration of different types of slurries.

References:

1. Ahmad Elkholy, (1983), “**Prediction of abrasive wear for slurry pump materials**”, Wear, Vol. 84, pp 39-49.
2. Andrews D.R. and Horsfield N, (1983), “**Particle collisions in the vicinity of an eroding surface**”, Journal of Physics, Vol. 16, pp. 525-538.
3. Shook C.A., McKibben M., and Small M., (1990), “**Experimental Investigation of some hydrodynamic factors affecting slurry pipeline wall erosion**”, Journal Chemical Engineering, Vol. 68, pp. 17-23.
4. Singh, T., Tiwari, N., and Sundararajan, G, (1991), “**Room temperature erosion behavior of 304, 316, and 410 stainless steels**”, Wear, Vol. 145, pp. 77-100.
5. Randall S. Lynn, Kien K. Wong, Hector McI. Clark, (1991), “**On the particle size effect in slurry erosion**”, Wear, Vol. 149, pp. 55-71.
6. Miller, J.D. and J.E. Miller, (1993), “**Solids concentration profiles and pressure drop in pipeline flow of multisized particulate slurries**”, International Journal of Multiphase Flow, Vol 28, pp 1697–1717.
7. Rajat Gupta, S.N. Singh, V.Seshadri(1994), “**Prediction of uneven wear in a slurry pipeline on the basis of pot tester**”.
8. Yuan Zhong, Kiyoshi Minemura,(1995) “**Numerical prediction of erosion wear in pump casing under solid water two phase flow**” Elsevier ,
9. Yoshiro Iwai a Kazuyuki Nambu,(1997)“**Slurry wear properties of pump lining materials** ” Wear, Vol 210, pp 211-219
10. R. Dasgupta, OP Modi, BK Parsad,(1998) “**Effects of sand concentration on slurry erosion of steels.**” Materials Transactions, JIM, Vol.39, pp 1885-1190.
11. Y. Xie, H. McI. Clark, H. M. Hawthorne,(1999), “**Modelling slurry particle dynamics in the Coriolis erosion tester**” Wear, Vol 225-229, Part 1, pp 405-416
12. B.K. Gandhi, S.N. Singh, V. Seshadri,(1999) “**Study of the parametric dependence of erosion wear for the parallel flow of solid–liquid mixtures**” Tribology International Vol 32, pp 275–282.
13. Y. Xie, H. McI. Clark, H. M. Hawthorne,(1999) “**Modelling slurry particle dynamics in the Coriolis erosion tester**” Wear, Vol 225-229, Part 1, pp 405-416.

14. Craig I. Walker, Greg C. Bodkin,(2000),“**Erosion of a High-Carbon Steel in Coal and Bottom-Ash Slurries Measurements of specific energies for erosive wear using a Coriolis erosion tester**” *Wear*, Vol 241, 1, pp1-9.
15. Abbade, N.P. and Crnkovic, S.J., (2000)“**Sand-water slurry erosion of API 5L X65 pipe steel as quenched from intercritical temperature.**” *Tribology International* Vol 33,pp 811-816.
16. Hawthorne H.M. (2002), “**Some Coriolis slurry erosion test developments**”, *Tribology International*, Vol. 35 ,pp 625–630.
17. Clark H. McI. (2002), “**Particle velocity and size effects in laboratory slurry erosion measurements or do you know what your particles are doing**”, *Tribology International*, Vol 35, pp 617–624.
18. Ghanta K.C. and Purohit N.K, (2002), “**Effect of Particle Size Distribution (PSD) on the Viscosity of Suspension of bi-dispersed Particles**”, *Proc. Hydrotransport 15*, BHR Group, Fluid Engineering, Cranfield, Bedford, England, pp. 299-313.
19. R.J.K.Wood,T.F.Jones (2004), “**Investigations of sand-water induced erosive wear of AISI 304L stainless steel pipes by pilot-scale and laboratory-scale testing**”.
20. Bhupendra K. Gandhi, Satish V. Borse,(2004)“**Nominal particle size of multi-sized particulate slurries for evaluation of erosion wear and effect of fine particles**”, *Wear*, Vol257,pp 73–79
21. A. Neville, F. Reza, S. Chiovelli, T. Revegab, (2005)“**Erosion–corrosion behaviour of WC-based MMCs in liquid–solid slurries**” *Wear*, Vol 259, pp181–195
22. Tian Harry H., Graeme R. Addie(2005), “**Experimental study on erosive wear of some metallic materials using Coriolis wear testing approach**”, *Journal of Wear* vol. 258 , pp 458–469.
23. Berget J., Rogne T., Bardal, (2007) “**Erosion-corrosion properties of different WC-Co-Cr coatings deposited by the HVOF process- influence of metallic matrix composition and spray powder size distribution.Surface and coating technology**”, pp 7619-7625.
24. T. Manisekaran, M. Kamaraj, S.M. Sharrif, and S.V. Joshi ,(2007) “ **Slurry Erosion Studies on Surface Modified 13Cr-4Ni Steels: Effect of Angle of Impingement and Particle Size.**”*JMEPEG*, pp567–572

25. .M.A. Al-Bukhaiti, S.M. Ahmedb, F.M.F. Badran b, K.M. Emarab,(2007) “**Effect of impingement angle on slurry erosion behaviour and mechanisms of 1017 steel and high-chromium white cast iron**” *Wear*, Vol 262, pp 1187–1198
26. William A. John, (2007), “ **Wear and wear particles-some fundamentals**”,*Tribology international*, 38 , Elsevier Science Journal.
27. Girish R. Desale, Bhupendra K. Gandhi , S.C. Jain,(2008) ,“**Slurry erosion of ductile materials under normal impact condition**” *Wear*, Vol 264, pp322–330
28. S.C.Mishra, S.Praharaj, Alok Satpathy,(2009) “**Evaluation of erosion wear of a ceramic coating with Taguchi approach**”. *Manufacturing Engineering*, Vol.4
29. Girish R. Desalea, Bhupendra K. Gandhi, S.C. Jain,(2009), “**Particle size effects on the slurry erosion of aluminium alloy (AA 6063)**”. *Wear* 266, pp1066–1071
30. H.H. Tian, G.R. Addie, R.J. Visintainer, (2009), “**Erosion–corrosion performance of high-Cr cast iron alloys in flowing liquid–solid slurries**” *Wear*, vol.267, 11, pp 2039-2047
31. Cunkui Huanga, P. Minevb, Jingli Luoc, K. Nandakumard,(2010)“**A phenomenological model for erosion of material in a horizontal slurry pipeline flow**”, *Wear*, Vol269, pp190–196